current issues in molecular biology

MDPI

Article

Physiological Responses and Gene Expression Analysis Associated with Exogenous Hydrogen Sulfide (H_2S)-Regulated Salt Tolerance in Maize Seedlings

Xinxin Xiang, Xiaoqiang Zhao *, Meiyue He, Jing Wang, Junmiao Long and Shangjie Yu

State Key Laboratory of Aridland Crop Science, College of Agronomy, Gansu Agricultural University, Lanzhou 730070, China; 18403693151@163.com (X.X.); hemeiyue0513@163.com (M.H.); 15138079530@163.com (J.W.); 15397202304@163.com (J.L.); ysj_0325@163.com (S.Y.)
* Correspondence: zhaoxiaoq@gsau.edu.cn; Tel.: +86-183-9415-8662

Abstract

Soil salinity severely restricts the growth and development of maize, even affecting its survival. Sodium hydrosulfide (NaHS), as a superior adjusting agent for alleviating salt stress, has attracted increasing attention. However, the effects of exogenous NaHS application on maize seedlings under salt stress are still unclear. Herein, maize seeds (M17-45-1 and M17-5-3) were primed by soaking with different concentrations of exogenous NaHS, and the resulting three-leaf stage seedlings were subsequently sprayed with the same NaHS solutions under 0 and 120 mM NaCl treatments. Seedlings were then assessed for growth status, physiological metabolism, and gene expression levels. Notably, the membership function and cluster analyses indicated that 75 μM NaHS was the most effective among the tested concentrations in alleviating 120 mM NaCl stress in maize seedlings under the present experimental conditions. Further physiological analysis revealed that, under 120 mM NaCl stress, the application of 75 μM NaHS significantly increased endogenous H_2S content (by 81.28% on average) and activities of superoxide dismutase (by 24.38% on average), peroxidase (by 52.79% on average), catalase (by 40.63% on average), and ascorbate peroxidase (by 20.00% on average) in the leaves of both maize genotypes. These enhancements effectively reduced reactive oxygen species accumulation, with $O_2^{\bullet-}$ level and H_2O_2 content decreasing by 12.80% and 15.21% on average, respectively. Moreover, the combined treatment of 75 μM NaHS and 120 mM NaCl significantly increased chlorophyll a (by 55.52% on average), b (by 19.84% on average), and carotenoid (by 14.65% on average) contents and net photosynthetic rate (by 13.57% on average), thereby clearly promoting the normal growth of maize seedlings. In addition, quantitative reverse transcriptase PCR (qRT-PCR) revealed that the expression of endogenous H_2S biosynthesis genes (*Zm00001d008187*, *Zm00001d043767*) and antioxidant-regulating genes (*Zm00001d009990*, *Zm00001d047479*, *Zm00001d040364*, *Zm00001d014848*, *Zm00001d007234*) was induced in maize seedlings under the combined treatment. Thus, these findings provide a foundation for understanding the roles of NaHS at key nodes in enhancing maize salt resistance.

Keywords: maize; NaCl stress; exogenous NaHS; antioxidant enzyme system; photosynthesis; H_2S biosynthesis; gene expression

Check for updates

Academic Editor: Zhaohui Chu

Received: 3 November 2026
Revised: 16 November 2026
Accepted: 23 November 2026
Published: 25 November 2026

Copyright: © 2026 by the authors. Licensee MDPI, Basel, Switzerland. This article is an open access article distributed under the terms and conditions of the Creative Commons Attribution (CC BY) license.

1. Introduction

The global extent of salt-affected soils is estimated at approximately 1.381 million hectares, representing nearly 20% of cultivated land, with productivity losses estimated

at 7–8% [1]. Owing to factors such as insufficient precipitation, high surface evaporation, rock weathering, improper irrigation practices, over-application of synthetic fertilizers, and poor agronomic management, an additional 1,038 million hectares are projected to become increasingly vulnerable to future salinization [1]. This will undoubtedly pose a huge challenge to sustainable agricultural production [2]. Sodium chloride (NaCl) is widely studied among researchers investigating osmotic, ionic, and oxidative stress under saline conditions due to its high solubility and ubiquitous distribution. Generally, different crop species cultivated in saline environments are subjected to osmotic stress and Na^+/Cl^- ion toxicity, resulting in exacerbated cell lipid peroxidation and boosting reactive oxygen species (ROS) [3]. This oxidative stress disrupts the antioxidant enzyme defense system, comprising superoxide dismutase (SOD), peroxidase (POD), catalase (CAT), and ascorbate peroxidase (APX) [4], and perturbs non-enzymatic antioxidants, such as ascorbic acid (ASA), glutathione (GSH), and phenolic acids (PAS) [5]. These disruptions lead to nutrient imbalance and irreversible cell damage [6]. As Li et al. have demonstrated, salt stress activates antioxidant enzyme activity and promotes flavonoid formation in peanuts (*Arachis hypogaea* L.), thereby protecting cells and eliminating excess ROS; concurrently, salt stress leads to a reduced seed germination rate, inhibited seedling growth, yield loss, and diminished crop quality [7]. When rice (*Oryza sativa* L.) plants were subjected to salt stress during the seedling stage, their growth was significantly restricted, resulting in a lower leaf area index; for salt-sensitive genotypes, the yield reduction was 15.3% greater than that of salt-tolerant types [8,9].

As one of the world's main food crops, maize (*Zea mays* L.) is a typical C_4 metabolism cereal crop that plays an irreplaceable role in economic development and national food security, and it is classified as a moderately sensitive plant to salinity. Therefore, protecting the maize growth environment has become a primary strategic requirement [10]. At the seedling stage, salt tolerance varies significantly among crop species. The near-lethal NaCl concentration for maize was determined to be approximately 250 mM [11], which was much lower than for winter rye (*Secale cereale* L.), whose semi-lethal NaCl concentration was as high as 408.69 mM [12]. Treatment with 120 mM NaCl stress can significantly inhibit the growth and development of maize seedlings, and with increasing stress time and concentration, the growth rate, root length, aboveground biomass, chlorophyll content, and leaf water content of seedlings show slowing or decreasing trends [13]. Furthermore, under NaCl stress, maize plants exhibit disrupted ionic homeostasis, as reflected by an altered Na^+/K^+ ratio. This imbalance subsequently affects nutrient uptake and assimilation, impairs the function of various enzymes, inhibits photosynthetic activity, and ultimately leads to premature senescence [14–16]. Because elite salt-tolerant maize varieties are extremely limited, investigating the salt tolerance of maize is of the utmost urgency.

Hydrogen sulfide (H_2S) is the 3rd gas signal molecule after carbon monoxide (CO) and nitric oxide (NO), and it has received attention in plant-related research in recent years [17]; however, H_2S is difficult to store and use. At present, the latest research on sodium hydrosulfide (NaHS, a donor of H_2S) highlights its involvement in various physiological processes, such as promoting root organogenesis, regulating stomatal movement and photosynthesis, as well as enhancing plant growth, development, and stress resistance capabilities [18]. Among studies on the responses to salt stress, Daneshvand et al. reported that 100 and 200 μM exogenous NaHS application enhanced the antioxidant defense and biochemical resilience of *Lavandula angustifolia* Mill under multiple NaCl stresses (0, 150, and 300 mM) for 7 and 14 days [19]. As pointed out in previous studies on wheat (*Triticum aestivum* L.), exogenous NaHS acts as an H_2S donor that promotes seed germination and mitigates copper toxicity in plants [20]. Exogenous NaHS application also significantly promotes endogenous H_2S generation in plants by inducing *L-cysteine desulfhydrase* (*LCD*) and *D-cysteine*

desulfhydrase (*DCD*) gene expression and by enhancing the activities of their enzymes, which are key players in endogenous H_2S synthesis [21]. Moreover, H_2S also exhibits a hormetic effect in plants. For example, a study on the *Arabidopsis lcd1* mutant showed that H_2S alleviated salt stress through auxin signaling [22]. Considering the challenges faced by maize under salinity stress, it remains unclear at what concentration exogenous NaHS can most effectively alleviate the negative effects of salt stress and through which mechanisms this alleviation occurs. Herein, seven different exogenous NaHS concentrations were used to spray two elite maize genotype (M17-45-1 and M17-5-3) seedlings under 120 mM NaCl stress. The aims of the study are to determine the optimal H_2S concentration for alleviating salt stress in maize seedlings and to elucidate the underlying physiological mechanisms and the transcriptional regulation of key genes in response to optimal exogenous NaHS treatment. Collectively, these results lay the groundwork for elucidating how NaHS contributes to salt tolerance in maize.

2. Materials and Methods

2.1. Maize Materials and Experimental Design

Two superior maize inbred lines, i.e., M17-45-1 and M17-5-3 originating from the Lancaster group, exhibit excellent yield performance and high combining ability, with contrasting salt stress responses. Their high-vigor seeds were produced at the Gansu Longxi experimental station, Gansu Province, China (34.97° N, 104.40° E, 2074 m altitude), in 2025, and were used for following experiments. The seeds of M17-45-1 and M17-5-3 were first surface-disinfected with 0.5% (v/v) sodium hypochlorite (NaClO) solution for 10 min, rinsed five times with double-distilled water (ddH_2O) to remove the residual disinfectant, and then primed by soaking in one of the following solutions: ddH_2O, 120 mM NaCl, or NaHS at 25, 50, 75, 100, 125, or 150 μM. These chemical reagents were purchased from Aladdin Biochemical Technology Co., Ltd. (Shanghai, China). All priming treatments were conducted at 20 ± 0.5 °C for 24 h. To sum up, the priming concentration varied among treatments, whereas the soaking duration and temperature were kept constant. Simultaneously, two sowing substrates were prepared by uniformly mixing 200 g of sterilized vermiculite with 200 mL NaCl solutions at two concentrations, yielding a non-saline substrate (SSWN, 0 mM NaCl) and a saline substrate (SSCN, 120 mM NaCl), respectively. Each substrate was then placed into plastic pots (11 cm diameter × 13 cm height). Ten primed seeds from the ddH_2O soaking treatment were sown in pots with SSWN, while ten primed seeds from each of the 120 mM NaCl and six NaHS concentration soaking treatments were sown in pots with SSCN. The sowing depth was maintained at 3 cm. Subsequently, all plots were placed in a HYR-600-EC intelligent artificial climate chamber (Shanxi Huayi Instrument Co., Ltd., Yangling, China). The cultivation conditions were set as a 12/12 h light/dark cycle, a constant temperature of 20 ± 0.5 °C, a light intensity of 300 μmol m^{-2} s^{-1}, and a relative humidity of 60%. Seven days after germination, the seedlings in each pot were irrigated with 50 mL ddH_2O every 2 days and foliar-sprayed with NaHS solution at different concentrations [i.e., 0 (ddH_2O), 25, 50, 75, 100, 125, or 150 μM], at 2 mL per seedling (20 mL per pot in total). After eight days of treatment (i.e., at the three-leaf stage), traits were measured. Overall, a total of eight treatments were established in this experiment, including CK, NaCl, NaCl+25NaHS, NaCl+50NaHS, NaCl+75NaHS, NaCl+100NaHS, NaCl+125NaHS, and NaCl+150NaHS (Table 1). Each treatment had three biological replicates. Based on comprehensive evaluations of both hierarchical cluster heatmaps and membership function analyses of 15 traits—seedling length (SL), stem diameter (SD), fresh weight of seedlings (SFW), root length (RL), fresh weight of roots (RFW), relative electrical conductivity (REC), relative water content (RWC), relative chlorophyll content (SPAD) value, chlorophyll a (Chl a) content, chlorophyll b (Chl b) content, carotenoid (Car) content, net photosynthetic

rate (Pn), stomatal conductance (Gs), transpiration rate (Tr), and intercellular CO_2 concentration (Ci)—in both maize genotypes under different treatments, 75 μM NaHS was successfully determined to be the optimal application concentration for alleviating 120 mM NaCl stress were (Figure 1A–D). Notably, these observed physiological and biochemical responses reflected the combined effects of the priming and foliar treatments rather than the effect of foliar NaHS application alone.

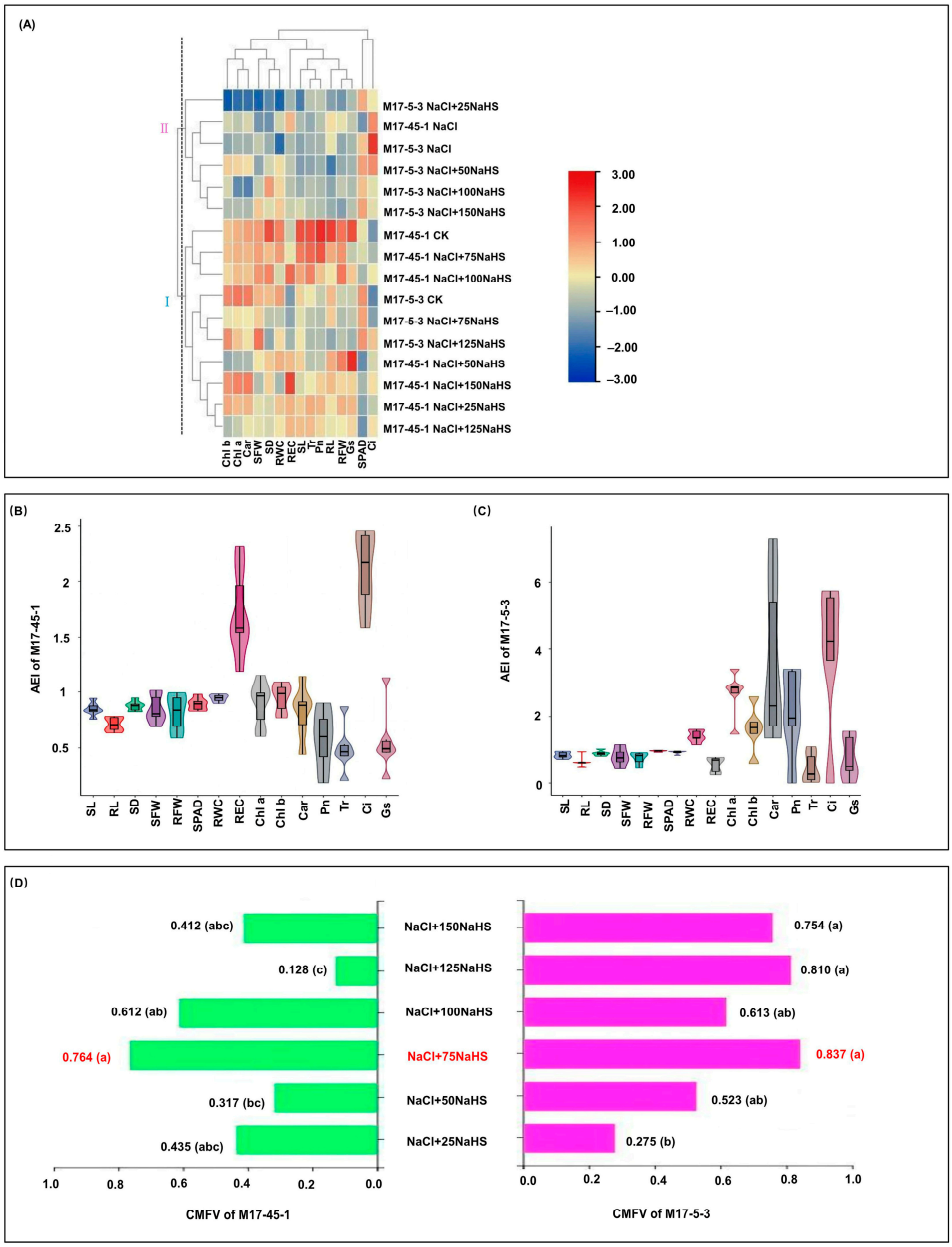

Figure 1. Hierarchical cluster heatmap analysis and membership function-based comprehensive evaluation of two maize genotypes under eight treatments. (**A**) Hierarchical cluster heatmap analysis. (**B**) Alleviation effect index (AEI) of applying different NaHS concentrations across 15 measured traits in M17-45-1 seedlings. (**C**) Alleviation effect index (AEI) of applying different NaHS concentrations across 15 measured traits in M17-5-3 seedlings. (**D**) The comprehensive alleviation effects on M17-45-1 and M17-5-3 seedlings under different NaCl+NaHS treatments, expressed as comprehensive membership function values (CMFVs). Car: carotenoid content; Chl a: chlorophyll a content; Chl b: chlorophyll b content; Ci: intercellular CO_2 concentration; Gs: stomatal conductivity; Pn: net photosynthetic rate; REC: relative electrical conductivity; RFW: root fresh weight; RL: root length; RWC: relative water content; SD: stem diameter; SFW: seedling fresh weight; SL: seedling length; SPAD:

relative chlorophyll content; Tr: transpiration rate. Different lowercase letters indicate significant differences among various treatments within the same maize genotype according to ANOVA at the $p < 0.05$ level.

Table 1. Experimental treatment scheme.

Treatment	Seed Soaking	Sowing Substrate	Foliar Spraying (Dosage)
CK	ddH_2O	Non-saline substrate (SSWN; uniformly mixing 200 g sterilized vermiculite with 0 mM NaCl)	ddH_2O (Sprayed with 20 mL at 2-day intervals)
NaCl	120 mM NaCl	Saline substrate (SSCN; uniformly mixing 200 g sterilized vermiculite with 1.404 g NaCl)	ddH_2O (Sprayed with 20 mL at 2-day intervals)
NaCl+25NaHS	25 μM NaHS	Saline substrate (SSCN; uniformly mixing 200 g sterilized vermiculite with 1.404 g NaCl)	25 μM NaHS (Sprayed with 20 mL at 2-day intervals)
NaCl+50NaHS	50 μM NaHS	Saline substrate (SSCN; uniformly mixing 200 g sterilized vermiculite with 1.404 g NaCl)	50 μM NaHS (Sprayed with 20 mL at 2-day intervals)
NaCl+75NaHS	75 μM NaHS	Saline substrate (SSCN; uniformly mixing 200 g sterilized vermiculite with 1.404 g NaCl)	75 μM NaHS (Sprayed with 20 mL at 2-day intervals)
NaCl+100NaHS	100 μM NaHS	Saline substrate (SSCN; uniformly mixing 200 g sterilized vermiculite with 1.404 g NaCl)	100 μM NaHS (Sprayed with 20 mL at 2-day intervals)
NaCl+125NaHS	125 μM NaHS	Saline substrate (SSCN; uniformly mixing 200 g sterilized vermiculite with 1.404 g NaCl)	125 μM NaHS (Sprayed with 20 mL at 2-day intervals)
NaCl+150NaHS	150 μM NaHS	Saline substrate (SSCN; uniformly mixing 200 g sterilized vermiculite with 1.404 g NaCl)	150 μM NaHS (Sprayed with 20 mL at 2-day intervals)

Similarly, a subsequent verification experiment was performed using independently grown plants in a separate experimental run. The disinfected seeds of M17-45-1 and M17-5-3 were soaked in ddH_2O, 120 mM NaCl, and 75 μM NaHS at 20 ± 0.5 °C for 24 h, respectively. The corresponding ten soaked seeds were then sown in plastic plots containing SSWN and SSCN, respectively. The cultivation conditions were identical to those described above (12/12 h light/dark cycle, 20 ± 0.5 °C, 300 μmol m^{-2} s^{-1}, 60% relative humidity). Seven days after germination, the seedlings of M17-45-1 and M17-5-3 in each pot were irrigated with 50 mL ddH_2O every 2 days and foliar-sprayed with NaHS solution at two concentrations [0 (ddH_2O) and 75 μM)] at 2 mL per seedling (20 mL per pot in total). After eight days of treatment (i.e., at the three-leaf stage), multiple growth phenotypes, biochemical traits, chlorophyll level, photosynthetic parameters, and gene expression levels were assayed in M17-45-1 and M17-5-3 seedlings. Thus, three treatments—CK, NaCl, and NaCl+75NaHS—were included in this experiment. Each treatment comprised three independent pots (biological replicates), with ten seedlings per pot.

2.2. Morphological and Physiological Analysis

The seedlings of M17-45-1 and M17-5-3 at the 3rd-leaf stage under different treatments were quickly rinsed with ddH_2O, and 3 seedlings with similar growth were selected to measure the seedlings' morphological characteristics, including SL, RL, SFW, and RFW. The leaves of corresponding seedlings under the three treatments were then immediately frozen in liquid nitrogen and stored at −80 °C for physiological analysis.

Using a multifunctional microplate reader (Syner622 gyHTX; BioTek Instruments, Winooski, VT, USA), physiological indicators were determined with commercial Solar biochemical test kits (Solar, Beijing, China). Briefly, 0.1 g of fresh leaf samples was homogenized in 1 mL of the corresponding extraction buffer under ice-bath conditions, the homogenate was centrifuged at 12,000 rpm for 10 min at 4 °C (Centrifuge 5425/5425 R; Eppendorf, Hamburg, Germany), and then the supernatant was collected for assay. The superoxide anion ($O_2^{\bullet-}$) content (Cat: BC1290) was determined by measuring the absorbance at 530 nm and was expressed as μM g^{-1} FW (fresh weight). The hydrogen peroxide (H_2O_2) content (Cat: BC3595) was determined by measuring the absorbance at 415 nm and was expressed as μM g^{-1} FW. The SOD activity (Cat: BC5165) was assayed by measuring the absorbance at 560 nm and was expressed as U g^{-1} FW. The POD activity (Cat: BC0095) was determined by measuring the absorbance at 470 nm and was expressed as U g^{-1} FW. The CAT activity (Cat: BC5855) was determined by measuring the absorbance at 240 nm and was expressed as U g^{-1} FW. The APX activity (Cat: BC0225) was assayed by measuring the absorbance at 290 nm and was expressed as U g^{-1} FW.

The SPAD value was estimated using a chlorophyll meter (SPAD-502 Plus, Konica Minolta, Japan). The four photosynthetic parameters, including net photosynthetic rate (Pn), intercellular CO_2 concentration (Ci), stomatal conductance (Gs), and transpiration rate (Tr), were measured using a LI-6800XT portable photosynthesis system (LI-COR; Lincoln, NE, USA, Bioscience Co., Ltd., Seongsouth-si, Republic of Korea) between 9:00 and 11:00. The leaf chamber was set to a photosynthetic photon flux density of 1000 μmol m^{-2} s^{-1}, a CO_2 concentration of 400 μmol mol^{-1}, and a leaf temperature of 25 °C. The chamber airflow rate was set to 600 μmol s^{-1} with the mixing fan set at 10,000 rpm. Measurements were recorded after the gas exchange parameters had stabilized (coefficient of variation < 1% over a 30 s interval), with three consecutive readings recorded and averaged per leaf.

The contents of three photosynthetic pigments, i.e., chlorophyll a (Chl a), chlorophyll b (Chl b), and carotenoid (Car), were determined using the method of Zhao et al. [23]. Briefly, 0.1 g of fresh leaves from M17-45-1 and M17-5-3 seedlings was weighed, soaked in 10 mL of 95% (*v*/*v*) ethanol for 48 h, and then centrifuged at 12,000 rpm for 10 min (Centrifuge 5425/5425 R; Eppendorf, Hamburg, Germany). Absorbance was measured at 665 nm, 649 nm, and 470 nm using a multifunctional microplate reader (Synergy HTX; Bio Tek Instruments, Inc., Winooski, VT, USA). The concentrations of Chl a (C_{ac}), Chl b (C_{bc}), and Car (C_{cc}) were calculated as follows:

$$C_{ac} = 13.95 \times A_{665} - 6.88 \times A_{649} \quad (1)$$

$$C_{bc} = 24.96 \times A_{649} - 7.32 \times A_{665} \quad (2)$$

$$C_{cc} = 1000 \times A_{470} - 2.05 \times C_{ac} - 114.8 \times C_{bc} \quad (3)$$

where C_{ac}, C_{bc}, and C_{cc} are expressed in mg L^{-1}. The photosynthetic pigment contents on a fresh weight basis were then calculated as follows:

$$\text{Chl a content (mg } g^{-1} \text{ FW)} = C_{ac} \times V_t \times n/FW \times 1000 \quad (4)$$

$$\text{Chl b content (mg } g^{-1} \text{ FW)} = C_{bc} \times V_t \times n/FW \times 1000 \quad (5)$$

$$\text{Car content (mg } g^{-1} \text{ FW)} = C_{cc} \times V_t \times n/FW \times 1000 \quad (6)$$

where FW is the fresh weight (g), V_t is the total volume of the extract (mL), and n is the dilution coefficient. The factor 1000 converts mL to L, so that the final content is expressed as mg g^{-1} FW.

Leaf FW of fully mature leaves was measured immediately after collection based on the method proposed by Ritchie et al. [24]. Afterward, the leaves were placed in distilled

water at 4 °C for 24 h to determine the turgor weight (TW). In the next stage, samples were dried in an oven at 70 °C for 48 h, and the dry weight (DW) of each sample was recorded. The percentage of relative water content (RWC) was estimated as follows:

$$\text{RWC} = [(\text{FW} - \text{DW})/(\text{TW} - \text{DW}) \times 100] \quad (7)$$

The relative electrolyte leakage (REC) was determined according to the method of Khampookhiaw et al. [25]. Briefly, leaf samples were washed with tap water, rinsed three times with distilled water, and blotted dry with filter paper. The leaves were then cut into small, uniform pieces, and a 0.1 g subsample was placed in a 10 mL graduated glass test tube filled with 10 mL deionized water. The test tube was covered with a glass plug and left to undergo immersion treatment at room temperature for 12 h. The conductivity (R_1) was measured at room temperature using a conductivity meter (DDSJ–319L, Shanghai, China). The test tube was then placed in a boiling water bath for 30 min, cooled to room temperature, and the conductivity (R_2) was measured. The relative electrolyte leakage (REC) was calculated as follows:

$$\text{REC} = (R_1/R_2) \times 100\% \quad (8)$$

Endogenous H_2S content was determined according to the method described by Yang et al. [5] with slight modifications. Briefly, 0.2 g of fresh leaves was homogenized in 5 mL of extraction buffer consisting of 50 mM phosphate buffer (pH 6.8) supplemented with 0.2 M ascorbic acid (ASA), 0.1 M ethylenediaminetetraacetic acid (EDTA), and 0.5 mL of 1.0 M hydrochloric acid (HCl). The concentrations of ASA and EDTA followed the original protocol, in which ASA and EDTA serve to prevent oxidation of sulfide during extraction and HCl drives the release of H_2S from acid-labile sulfur pools. The released H_2S was trapped immediately by the addition of 1.0% (*w*/*v*) zinc acetate. Next, 0.3 mL of 5 mM N,N-dimethyl-p-phenylenediamine dissolved in 3.5 mM sulfuric acid (H_2SO_4) and 0.3 mL of 50 mM ammonium ferric sulfate were sequentially added to the trapped solution, giving a final reaction volume of approximately 1.1 mL. Following a 15 min dark incubation at room temperature, the absorbance was measured at 667 nm using a Shimadzu UV-1280 spectrophotometer (Shimadzu Corp., Kyoto, Japan). The standard curve was constructed using graded concentrations of $Na_2S{\cdot}9H_2O$ solution. Three biological replicates were performed for each treatment, and the endogenous H_2S content was expressed as nM g^{-1} FW. Notably, to minimize interference from the NaHS foliar treatment, all leaf samples were thoroughly rinsed with deionized water prior to homogenization, and sampling was performed at least 24 h after the final NaHS application.

2.3. Primer Design and Antioxidant Enzyme-Related Gene Expression Analysis

According to previous studies [5,26,27], five antioxidant-regulating genes and two H_2S biosynthesis-related genes were selected for relative expression analysis via quantitative reverse transcriptase PCR (qRT-PCR) in seedlings of the two maize genotypes under the three treatments. Total RNA was extracted from leaf samples using a plant RNA extraction kit (Solarbio, Beijing, China) according to the manufacturer's instructions. RNA concentration and purity were assessed using a microvolume spectrophotometer. RNA integrity was verified via 1% agarose gel electrophoresis. Residual genomic DNA was removed by treatment with RNase-free DNase I prior to reverse transcription. First-strand cDNA was synthesized from 1 μg of total RNA in a 20 μL reaction using a reverse transcription kit according to the manufacturer's protocol. *Zm00001d010159* (*Actin-1*) and *Zm00001d049641* (*GAPDH*) served as the internal reference genes [28–30]. Specific primers were designed using the NCBI Primer-BLAST design tool (https://www.ncbi.nlm.nih.gov/tools/primer-blast/; viewed on 19 March 2026) (Table 2). qRT-PCR was conducted on a Light Cycler 480II fluorescence

quantitative PCR instrument (Roche, Munich, Germany) in a 20 µL reaction mixture containing 10 µL of SYBR Green Master Mix, 0.5 µL of each primer (10 µM), 2 µL of diluted cDNA, and 7 µL of nuclease-free water. Relative expression levels were calculated using the $2^{-\Delta\Delta CT}$ method [23], with normalization performed separately against each reference gene (*Actin-1* and *GAPDH*), and each treatment was analyzed in three biological replicates.

Table 2. Sequences of primers used in quantitative reverse transcriptase PCR (qRT-PCR) of eight candidate genes.

Gene ID	Encoding Protein	Reference	Chromosome	Primer Sequence (5′ to 3′)
Zm00001d008187	L-cysteine desulfhydrase1 (LCD1)	[5]	8	Forward: AAGGGCGATCAAGTGACAGG Reverse: AGAAGGTCTCAGCTTGGTGC
Zm00001d043767	D-cysteine desulfhydrase 2 (DCD2)	[5]	3	Forward: TCCAGTGGAGGGTTACTGCT Reverse: AAACCGCTCCACCCATTGAA
Zm00001d009990	Superoxide dismutase [Mn] 3.4 (SOD3.4)	[26]	8	Forward: GATGAATGCAGAAGGCGCTG Reverse: TACGCATGCTCCCAGACATC
Zm00001d047479	superoxide dismutase [Cu-Zn] 4A (SOD4A)	[26]	9	Forward: TTGGTAGCAGCGATGGTGTC Reverse: CTCCTTGCTCGCAGGATTGT
Zm00001d014848	catalase 1 (CAT1)	[26]	5	Forward: ACAGGCTGTCGTGAGAAGTG Reverse: TACGGTGTTCATGGGTCACG
Zm00001d040364	peroxidase 72 (POD72)	[27]	3	Forward: GGATGTATCCTACGCCGCAA Reverse: TTGTCAAACTTGGCAGGGGT
Zm00001d007234	ascorbate peroxidase 2 (APX2)	[26]	2	Forward: TGGGAAGATGCCACAAGGAC Reverse: ACTTGGTAGCTGCAGAAGGC
Zm00001d010159	Actin-1	[28]	8	Forward: CGATTGAGCATGGCATTGTCA Reverse: CCCACTAGCGTACAACGAA
Zm00001d049641	GAPDH	[30]	4	Forward: ATCAACGGCTTCGGAAGGAT Reverse: CCGTGGACGGTGTCGTACTT

2.4. Alleviation Effect Index (AEI) and Membership Function-Based Comprehensive Evaluation

To comprehensively evaluate the alleviation effect of applying various NaHS concentrations on each measured trait under 120 mM NaCl stress, the alleviation effect index (AEI) was calculated as follows [29]:

$$AEI_{m\text{-}(NaCl+nNaHS)} = [X_{m\text{-}(NaCl+nNaHS)} - X_{m\text{-}(CK)}]/|[X_{m\text{-}(CK)} - X_{m\text{-}(NaCl)}]| \times 100\% \quad (9)$$

$$AEI_{m\text{-}(NaCl+nNaHS)} = [X_{m\text{-}(CK)} - X_{m\text{-}(NaCl+nNaHS)}]/|[X_{m\text{-}(CK)} - X_{m\text{-}(NaCl)}]| \times 100\% \quad (10)$$

where $AEI_{m\text{-}(NaCl+nNaHS)}$ is the alleviation effect index of applying the n-th (n = 25, 50, 75, 100, 125, or 150) NaHS concentration on the m-th measured trait under 120 mM NaCl stress, $X_{m\text{-}(NaCl+nNaHS)}$ is the m-th measured trait under NaCl+nNaHS treatment, $X_{m\text{-}(CK)}$ is the m-th measured trait under CK treatment, and $X_{m\text{-}(NaCl)}$ is the m-th measured trait under NaCl treatment. Notably, the 15 measured traits were classified into two categories according to their expected direction of response to salinity and to NaHS alleviation. Traits for which higher values indicate better plant performance under salinity, i.e., SL, RL, SD, SFW, RFW, SPAD, RWC, Chla, Chl b, Car, Pn, Tr, and Gs, were defined as positive traits, and Equation (9) was used. Traits for which lower values indicate better performance, i.e., REC and Ci, were defined as negative traits, and Equation (10) was used. Subsequently, the membership function-based comprehensive evaluation was used to estimate the alleviation effect of applying various NaHS concentrations on each measured trait under 120 mM NaCl stress, as follows:

$$U_{m\text{-}(NaCl+nNaHS)} = [AEI_{m\text{-}(NaCl+nNaHS)} - AEI_{m\text{-}min}]/[AEI_{m\text{-}max} - AEI_{m\text{-}min}] \quad (11)$$

$$U_{m\text{-}(NaCl+nNaHS)} = 1 - [AEI_{m\text{-}(NaCl+nNaHS)} - AEI_{m\text{-}min}]/[AEI_{m\text{-}max} - AEI_{m\text{-}min}] \quad (12)$$

$$CMFV_{(NaCl+nNaHS)} = \Sigma U_{m\text{-}(NaCl+nNaHS)}/p \quad (13)$$

where $U_{m\text{-}(NaCl+nNaHS)}$ is the membership function value (MFV) of the AEI for the m-th measured trait under NaCl+nNaHS treatment, $AEI_{m\text{-}min}$ is the minimum value of AEI for the m-th measured trait under all NaCl+NaHS treatments, $AEI_{m\text{-}max}$ is the maximum value of AEI for the m-th measured trait under all NaCl+NaHS treatments, $CMFV_{(NaCl+nNaHS)}$ is comprehensive alleviation effect of NaHS on 120 mM NaCl stress under NaCl+nNaHS treatment, and p ($p = 15$) is the number of measured traits. When the m-th measured trait was positively associated with maize salt tolerance, Equation (11) was calculated; by contrast, the Equation (12) was calculated.

2.5. Statistical Analysis

All analyses were based on three independent biological replicates. Microsoft Excel 2016 was used to organize and summarize all data. All statistical analyses for the two maize genotypes under different treatments were performed using IBM-SPSS Statistics v.20.0 software (SPSS, Chicago, IL, USA; https://www.Ibm.com/products/spss-statistics; viewed on 10 January 2026). Factorial analysis of variance (genotype, treatment, and their interaction) were performed using the general linear model for univariate (GLM-univariate). Duncan's method was used to determine significant differences between treatments ($p < 0.05$), where different letters indicated significant differences. Hierarchical cluster heatmaps were plotted using https://www.bioinformatics.com.cn (viewed on 23 November 2025), an online platform for data analysis and visualization. Pearson correlation graphs of all traits in seedlings of the two maize genotypes under all treatments were drawn using the Origin 2021 (Version 21.0, Origin Pro, USA; https://www.originlab.com/2021; viewed on 1 April 2026).

3. Results

3.1. Differential Seedling Performance and Hierarchical Cluster Heatmap Analysis

The 15 traits, including SL, RL, SD, SFW, RFW, SPAD, RWC, REC, Chl a, Chl b, Car, Tr, Pn, Ci, and Gs, were measured in seedlings of the two maize genotypes (M17-45-1 and M17-5-3) across eight treatments (Table 1). A two-way analysis of variance (ANOVA) was then performed to test the effects of genotype (G), treatment (T), and their interaction (G × T) on each measured trait. The complete ANOVA results, including degrees of freedom (DF), *F*-values, and exact *p*-values for the G, T, and G × T effects on all 15 traits, are presented in Table S1, which revealed that all measured traits were significantly affected by genotype, treatment, and G × T interaction (Table S1). These findings demonstrate that the resistance to salt stress in maize seedlings is co-regulated by the above three sources. Therefore, it was essential to conduct a comprehensive evaluation and differential classification of salt tolerance in maize seedlings subjected to various treatments.

Interestingly, the hierarchical cluster heatmap analysis based on the above 15 measured traits found that the maize genotype seedlings under different treatments were clearly divided into two distinct types. The I type included M17-45-1 seedlings grown under NaCl+125NaHS, NaCl+25NaHS, NaCl+150NaHS, NaCl+50NaHS, NaCl+100NaHS, NaCl+75NaHS, and CK treatments, and M17-5-3 seedlings grown under NaCl+75NaHS, NaCl+125NaHS, and CK treatments. This grouping indicated that maize seedlings under these treatments suffered slight salt-induced damage or experienced no salt injury and exhibited better growth status. However, the II type showed a completely opposite trend, including M17-45-1 seedlings grown under NaCl treatment, and M17-5-3 seedlings grown under NaCl, NaCl+25NaHS, NaCl+50NaHS, NaCl+150NaHS, and NaCl+100NaHS treatments (Figure 1A). Moreover, the AEIs of applying different NaHS concentrations on the

above 15 measured traits in M17-45-1 and M17-5-3 seedlings under 120 mM NaCl stress were calculated (Figure 1B,C), and then the comprehensive alleviation effect was estimated by the comprehensive membership function value (CMFV), showing that under NaCl+75NaHS treatment, M17-45-1 and M17-5-3 seedlings exhibited the most pronounced comprehensive alleviation effects ($p < 0.05$), with CMFVs of 0.764 and 0.837, respectively (Figure 1D). In conclusion, under 120 mM NaCl stress, 75 μM NaHS application (i.e., NaCl+75NaHS treatment) significantly promoted seedling growth and improved the physiological characteristics of both maize genotypes. Thus, it was necessary to further elucidate the effects of the NaCl+75NaHS combined treatment on the physiological mechanisms and the expression levels of related regulating genes in seedlings of these two maize genotypes.

3.2. Phenotypic Changes in Two Maize Genotypes Under Different Treatments

The growth of seedlings of the two maize genotypes was significantly inhibited after being cultivated under 120 mM NaCl stress (Figure 2A–F; Table S2). Compared with CK, the maize seedlings of M17-45-1 and M17-5-3 exposed to 120 mM NaCl stress exhibited reductions in SL by 41.64% ($p < 0.05$) and 29.04% ($p < 0.05$), RL by 30.12% ($p < 0.05$) and 46.74% ($p < 0.05$), SFW by 58.84% ($p < 0.05$) and 41.39% ($p < 0.05$), RFW by 6.77% ($p > 0.05$) and 47.49% ($p < 0.05$), seedling dry weight (SDW) by 60.90% ($p < 0.05$) and 38.31% ($p < 0.05$), and root dry weight (RDW) by 43.42% ($p < 0.05$) and 48.25% ($p < 0.05$), respectively. Compared with 120 mM NaCl stress alone, the addition of 75 μM NaHS under 120 mM NaCl stress (NaCl+75NaHS treatment) significantly increased SL, SFW, and SDW by 28.42% ($p < 0.05$), 73.23% ($p < 0.05$), and 77.53% ($p < 0.05$) in M17-45-1 seedlings, respectively, while significantly increasing SL, RL, RFW, and RDW by 33.17% ($p < 0.05$), 11.70% ($p < 0.05$), 18.55% ($p < 0.05$), and 60.81% ($p < 0.05$) in M17-5-3 seedlings, respectively (Figure 2A–F; Table S2). These results indicate that applying 75 μM NaHS effectively alleviates salt-induced growth inhibition and maintains the normal growth and development of maize seedlings.

3.3. Oxidative Stress Responses of Two Maize Genotypes Under Different Treatments

Previous studies reported that oxidative stress can influence the salt stress tolerance of plants [31,32]. In this study, M17-45-1 and M17-5-3 seedlings were consistently in a state of oxidative stress when subjected to 120 mM NaCl stress. The $O_2^{\bullet-}$ content (16.82% and 42.91%; $p < 0.05$), the H_2O_2 content (13.83% and 96.62%; $p < 0.05$), and REC (37.63% and 34.40%; $p < 0.05$) of leaves in the seedlings of both maize genotypes significantly increased compared with non-stressed seedlings, respectively (Figure 3A–C). These results thus indicate that NaCl stress induces a burst of ROS in maize leaves, and this excessive ROS accumulation disrupts cell membrane lipids, resulting in enhanced membrane permeability and accelerated water loss [17]. Our results also support this view, as the RWC of leaves in M17-45-1 and M17-5-3 seedlings decreased by 29.12% ($p < 0.05$) and 26.87% ($p < 0.05$), respectively (Figure 3D). Interestingly, relative to the 120 mM NaCl treatment, the application of 75 μM NaHS to M17-5-3 seedlings under stress reduced leaf $O_2^{\bullet-}$ content (22.17%; $p < 0.05$), H_2O_2 content (23.47%; $p < 0.05$), and REC (9.09%; $p < 0.05$), while elevating leaf RWC (18.00%; $p > 0.05$) (Figure 3A–D). A similar pattern of variation was also observed in M17-45-1 leaves, where the NaCl+75NaHS treatment also caused a 3.44% ($p > 0.05$) decrease in $O_2^{\bullet-}$ content, a 6.94% ($p > 0.05$) decrease in H_2O_2 content, a 17.19% ($p < 0.05$) decrease in REC content, and a 32.03% ($p < 0.05$) increase in RWC in the leaves of M17-5-3 seedlings compared with 120 m M NaCl stress alone (Figure 3A–D). These findings thus highlight that 75 μM NaHS can alleviate salt-induced oxidative damage and membrane injury, and shows a tendency to improve leaf water status. Notably, NaHS also exerts genotype-dependent effects, and the genotypic differences in the ROS-scavenging and

water-maintenance capacities of NaHS may be associated with the extent of salt-induced damage in the genotypes themselves.

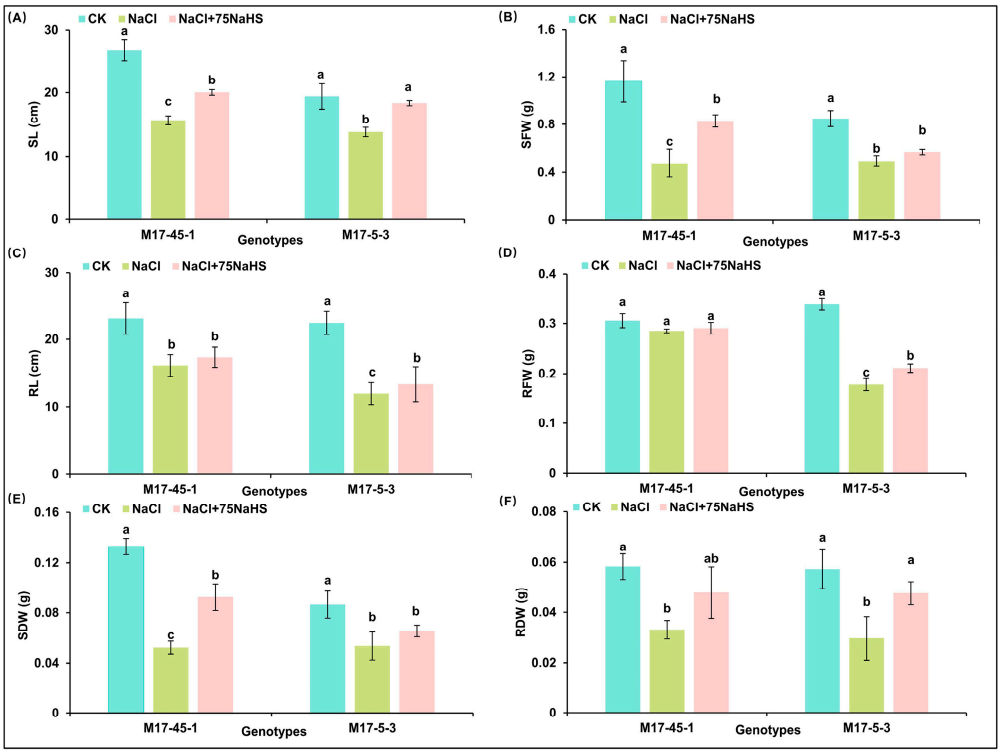

Figure 2. Phenotypic changes in seedlings of two maize genotypes (M17-45-1 and M17-5-3) under different treatments. (**A**) Changes in seedling height (SL). (**B**) Changes in seedling fresh weight (SFW). (**C**) Changes in root length (RL). (**D**) Changes in root fresh weight (RFW). (**E**) Changes in seedling dry weight (SDW). (**F**) Changes in root dry weight (RDW). Different lowercase indicate significant differences among various treatments within the same maize genotype according to ANOVA at $p < 0.05$ level, respectively.

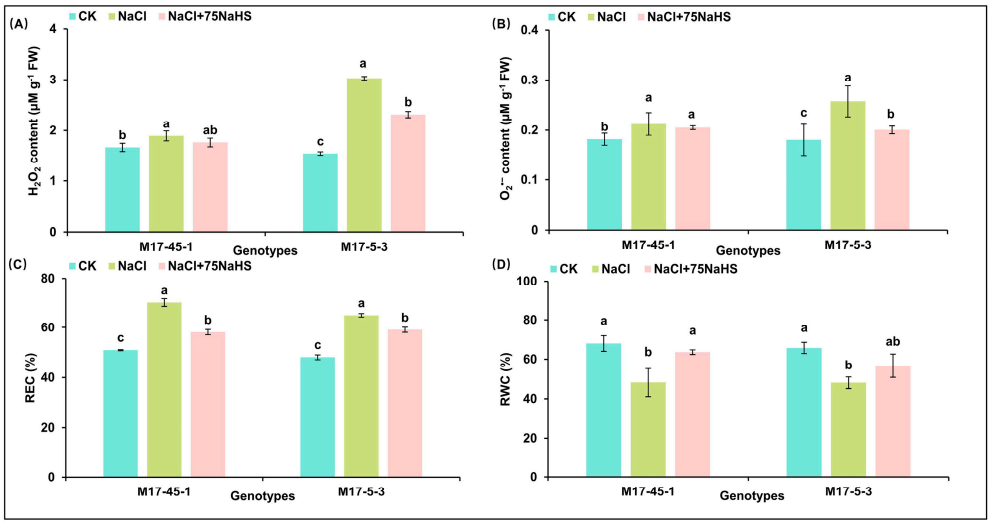

Figure 3. Changes in reactive oxygen species (ROS) and leaf moisture levels in seedlings of two maize genotypes (M17-45-1 and M17-5-3) under different treatments. (**A**) Changes in hydrogen peroxide (H_2O_2) content. (**B**) Changes in superoxide anion ($O_2^{\bullet-}$) content. (**C**) Changes in relative electrical conductivity (REC). (**D**) Changes in relative water content (RWC). Different lowercase letters indicate significant differences among various treatments within the same maize genotype according to ANOVA at the $p < 0.05$ level, respectively.

3.4. Chlorophyll and Photosynthesis Changes in Two Maize Genotypes Under Different Treatments

Chlorophyll (Chl) is indispensable to plants as the main pigment for capturing light energy during photosynthesis, which is the fundamental process for plant growth and biomass accumulation [33,34]. As a crucial energy converter and signal sensor, Chl not only drives the conversion of light energy into chemical energy, but also plays a vital role in regulating the response of plants to environmental stress [35]. In the present study, the contents of three photosynthetic pigments were measured in seedlings of the two maize genotypes under different treatments. Compared with the CK control, 120 mM NaCl stress significantly decreased leaf Chl a content (66.35% and 36.73%; $p < 0.05$), Chl b content (43.20% and 23.48%; $p < 0.05$), and Car content (50.81% and 33.63%; $p < 0.05$) in M17-45-1 and M17-5-3 seedlings (Figure 4A–C). These results indicate that salt stress exerts a comprehensive detrimental effect on the photosynthetic pigment system of maize seedlings. By contrast, when M17-45-1 and M17-5-3 seedlings were cultivated under the NaCl+75NaHS combined treatment, the leaf Chl a content (82.21% and 28.83%; $p < 0.05$), Chl b content (27.70% and 11.98%; $p < 0.05$), and Car content (2.94% and 26.41%; $p < 0.05$) were significantly increased compared with 120 mM NaCl stressed seedlings (Figure 4A–C). Therefore, these findings demonstrate that NaHS can effectively promote the accumulation of Chl and Car in maize seedling leaves under salt stress, thereby providing a pigment basis for the improved photosynthetic performance.

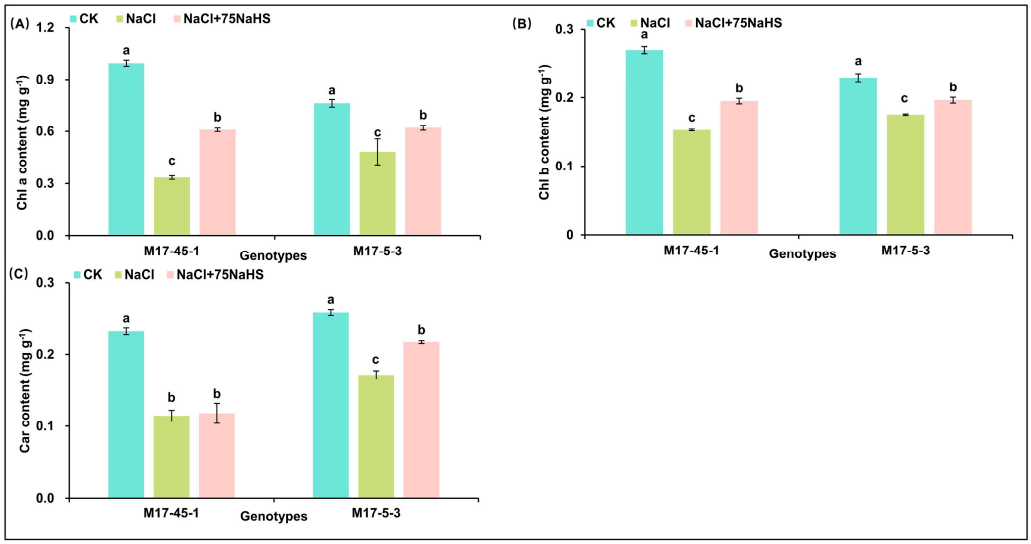

Figure 4. Changes in leaf photosynthetic pigments in seedlings of two maize genotypes (M17-45-1 and M17-5-3) under different treatments. (**A**) Changes in chlorophyll a (Chl a) content. (**B**) Changes in chlorophyll b (Chl b) content. (**C**) Changes in carotenoid (Car) content. Different lowercase letters indicate significant differences among various treatments within the same maize genotype according to ANOVA at the $p < 0.05$ level, respectively.

Moreover, the photosynthesis of maize seedlings was also highly sensitive to salt stress. For M17-45-1 and M17-5-3 seedlings cultivated under normal treatment, their key photosynthetic parameters, i.e., Pn (43.67% and 22.40%; $p < 0.05$), Gs (49.46% and 57.91%; $p < 0.05$), and Tr (41.93% and 11.13%; $p < 0.05$), exhibited significant declines under the 120 mM NaCl treatment (Figure 5A–D). This finding indicates that salt stress damages maize's photosynthetic system and inhibits organic matter accumulation. By contrast, the NaCl+75NaHS combined treatment resulted in pronounced enhancements in the photosynthetic parameters of M17-45-1 and M17-5-3 seedlings, significantly increasing Pn (by 10.72% and 39.83%; $p < 0.05$) and Gs (by 16.42% and 29.03%; $p < 0.05$) compared with 120 mM NaCl stress. The Tr response in M17-45-1 seedling leaves was not significant ($p > 0.05$),

whereas the Tr response in M17-5-3 seedling leaves exhibited a 6.19% increase ($p < 0.05$). Ci in M17-45-1 and M17-5-3 seedlings under the NaCl+75NaHS combined treatment significantly ($p < 0.05$) decreased by 24.34% and 25.12%, respectively, compared with 120 mM NaCl stress alone (Figure 5A–D). Therefore, we speculated that, similar to its effects on rice [36] and wheat [37] under NaCl stress, applying an appropriate concentration of NaHS could enhance photosynthetic capacity and consequently increase biomass and yield in maize grown under saline conditions.

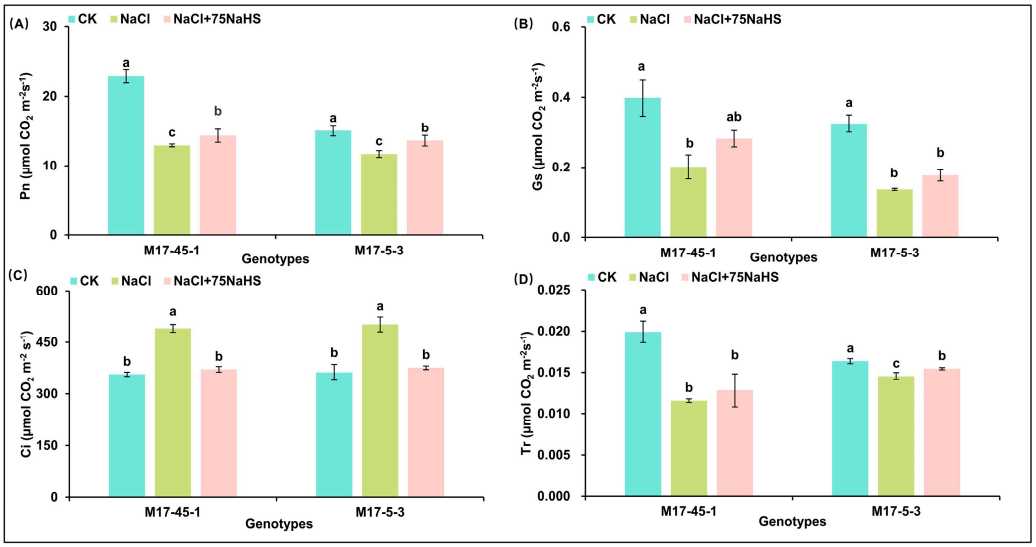

Figure 5. Changes in leaf photosynthetic parameters in seedlings of two maize genotypes (M17-45-1 and M17-5-3) under different treatments. (**A**) Changes in net photosynthetic rate (Pn). (**B**) Changes in stomatal conductance (Gs). (**C**) Changes in intercellular CO_2 concentration (Ci). (**D**) Changes in transpiration rate (Tr). Different lowercase letters indicate significant differences among various treatments within the same maize genotype according to ANOVA at the $p < 0.05$ level, respectively.

3.5. Antioxidant Enzymes and Regulating Gene Changes of the Two Maize Genotypes Under Different Treatments

In plants subjected to salt stress, antioxidant enzymes enhance the protective function of cells against oxidative stress [38–40]. In this study, compared with the CK environment, 120 mM NaCl stress caused varying enhancements in SOD activity (44.74% and 42.57%; $p < 0.05$), CAT activity (27.78% and 75.00%; $p < 0.05$), and APX activity (25.00% and 66.67%) in leaves of M17-45-1 and M17-5-3 seedlings, respectively, while POD activity in M17-45-1 leaves was significantly enhanced by 28.30% ($p < 0.05$) (Figure 6A–D). These data demonstrate that maize seedlings activate their own antioxidant defense system to adapt to salt tolerance. Differentially, under 120 mM NaCl stress, POD activity (20.00% and 85.57%; $p < 0.05$) in the leaves of M17-45-1 and M17-5-3 seedlings was significantly increased by 75 μM NaHS supply, while SOD activity (41.49%; $p < 0.05$), CAT activity (76.19%; $p < 0.05$), and APX activity (20.00%) in the leaves of M17-5-3 seedlings were clearly increased by 75 μM NaHS supply, respectively (Figure 6A–D). These results demonstrate that the enzymatic antioxidant system of M17-5-3 is more sensitive to NaHS. Meanwhile, the NaHS-induced increases in SOD, CAT, APX, and POD activities coincided with the significant decreases in $O_2^{\bullet-}$ level, H_2O_2 content, and REC observed earlier in M17-5-3 seedling leaves (Figure 3A–C), indicating that these enhanced enzyme activities are accompanied by reduced ROS accumulation and alleviated membrane damage rather than merely reflecting a stress response.

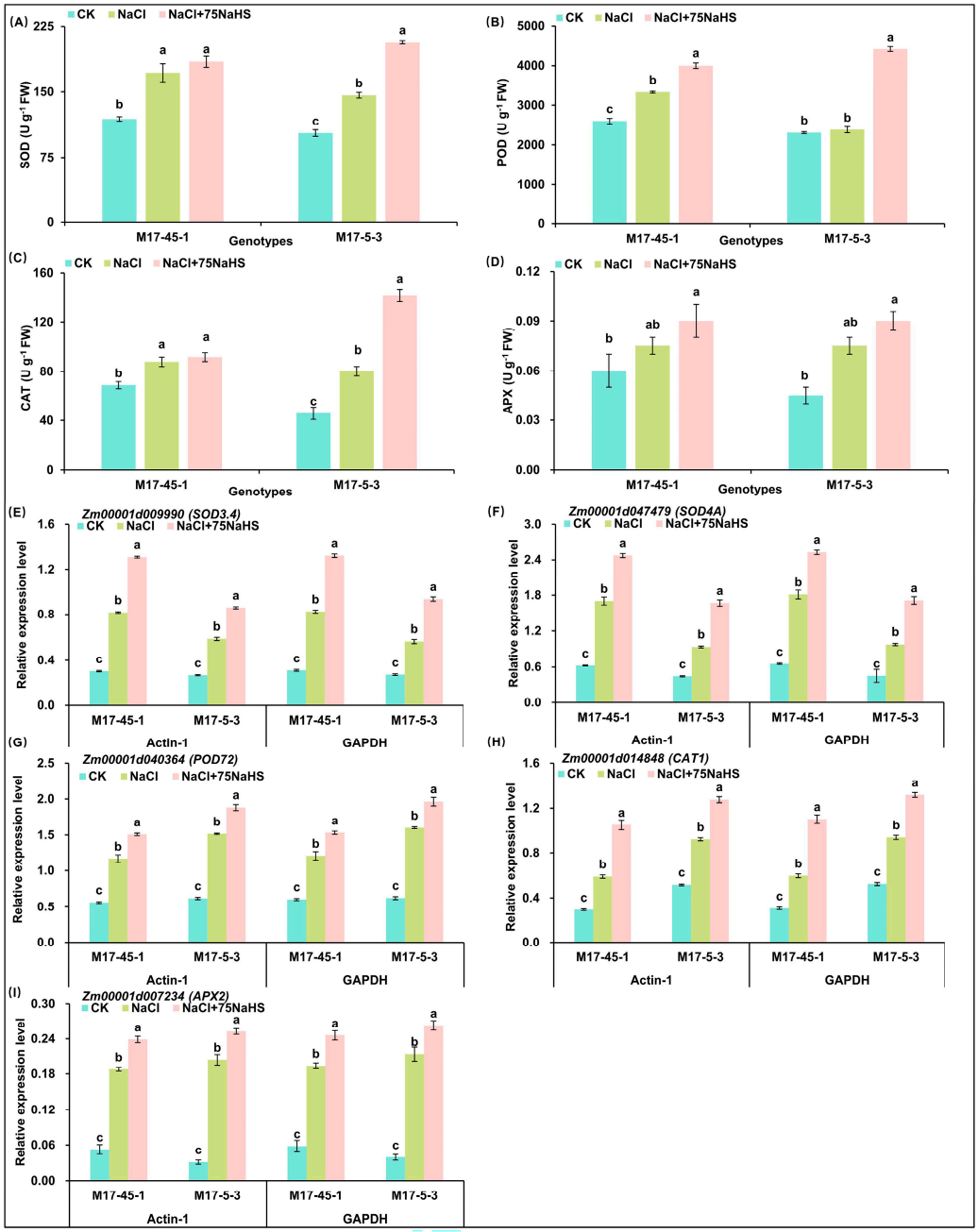

Figure 6. The changes in antioxidant enzyme activities and antioxidant-regulating gene expression levels in the leaves of the seedlings of two maize genotypes (M17-45-1 and M17-5-3) under different treatments. (**A**) Changes in superoxide dismutase (SOD) activity. (**B**) Changes in peroxidase (POD) activity. (**C**) Changes in catalase (CAT) activity. (**D**) Changes in ascorbate peroxidase (APX) activity. (**E**) *Zm00001d009990* (*SOD3.4*) expression level using the selected reference genes, including *Zm00001d010159* (*Actin-1*) and *Zm00001d049641* (*GAPDH*). (**F**) *Zm00001d047479* (*SOD4A*) expression level using the selected reference genes, including *Zm00001d010159* (*Actin-1*) and *Zm00001d049641* (*GAPDH*). (**G**) *Zm00001d040364*(*POD72*) expression level using the selected reference genes, including *Zm00001d010159* (*Actin-1*) and *Zm00001d049641* (*GAPDH*). (**H**) *Zm00001d014848*(*CAT1*) expression level using the selected reference genes, including *Zm00001d010159* (*Actin-1*) and *Zm00001d049641* (*GAPDH*). (**I**) *Zm00001d007234*(*APX2*) expression level using the selected reference genes, including *Zm00001d010159* (*Actin-1*) and *Zm00001d049641* (*GAPDH*). Different lowercase letters indicate significant differences among various treatments within the same maize genotype according to ANOVA at the $p < 0.05$ level, respectively.

Moreover, under these treatments, the relative expression levels of five antioxidant-regulating genes in M17-45-1 and M17-5-3 leaves showed consistent trends, although the absolute values differed slightly depending on the reference gene used (Figure 6E–I). To clarify the normalization strategy, each target gene was normalized separately against two reference genes, i.e., *Zm00001d010159* (*Actin-1*) and *Zm00001d049641* (*GAPDH*), and the two normalized datasets are presented separately in Figure 6E–I rather than being averaged. Fold changes were calculated relative to the CK for each reference gene, and the corresponding variability (mean ± SD of three independent biological replicates) is shown as error bars in Figure 6E–I. Compared with CK, the 120 mM NaCl stress and NaCl+75NaHS treatments significantly ($p < 0.05$) upregulated all five genes (Figure 6E–I). When normalized to *Actin-1* and *GAPDH*, respectively, the fold changes were as follows: *Zm00001d009990* (*SOD3.4*), 2.68 and 4.29 in M17-45-1 leaves, 2.13 and 3.33 in M17-5-3 leaves; *Zm00001d047479* (*SOD4A*), 2.75 and 3.91 in M17-45-1 leaves, 2.14 and 3.78 in M17-5-3 leaves; *Zm00001d040364* (*POD72*), 2.04 and 2.51 in M17-45-1 leaves, 2.61 and 3.10 in M17-5-3 leaves; *Zm00001d014848* (*CAT1*); 1.97 and 3.58 in M17-45-1 leaves, 1.79 and 2.50 in M17-5-3 leaves; and *Zm00001d007234* (*APX2*), 3.47 and 4.40 in M17-45-1 leaves, 6.08 and 7.49 in M17-5-3 leaves (Figure 6E–I). These results indicate that these antioxidant-related genes are responsive to NaCl stress and NaHS treatments, although whether they directly mediate the observed physiological changes requires further functional evidence.

3.6. Endogenous H_2S and H2S Biosynthesis-Related Genes Changes in the Two Maize Genotypes Under Different Treatments

H_2S is a critical endogenous gasotransmitter that mediates plant physiological regulation and stress responses [41]. Therefore, monitoring its dynamic changes in plants is crucial for understanding plant stress tolerance. In the current study, compared with the CK environment, the leaf endogenous H_2S content in M17-45-1 and M17-5-3 seedlings under 120 mM NaCl stress was significantly increased, with 74.10% ($p < 0.05$) and 84.92% ($p < 0.05$) increases, respectively (Figure 7A). This change may contribute to enhanced maize seedling adaptability to salt stress. The leaf endogenous H_2S level in M17-45-1 and M17-5-3 seedlings were further enhanced under the NaCl+75NaHS combined treatment, with 76.94% ($p < 0.05$) and 85.61% ($p < 0.05$) enhancements, respectively, compared with salt-stressed seedlings (Figure 7A). These results demonstrate that exogenous NaHS application can further stimulate the accumulation of endogenous H_2S in maize seedlings cultivated under NaCl stress conditions.

In addition, under these treatments, the relative expression levels of two H_2S biosynthesis-related genes exhibited consistent trends, although the absolute values differed slightly depending on the reference gene used (Figure 7B,C). Each target gene was normalized separately to the two reference genes, and fold changes were calculated relative to the CK for each reference gene (Figure 7B,C). Compared with non-stressed seedlings, both the 120 mM NaCl stress and NaCl+75NaHS treatments significantly ($p < 0.05$) up-regulated two H_2S biosynthesis-related genes (Figure 7B,C). When normalized to *Actin-1* and *GAPDH*, respectively, the fold changes were as follows: *Zm00001d008187* (*LCD1*), 1.41 and 1.40 in M17-45-1 leaves, 1.36 and 1.19 in M17-5-3 leaves; *Zm00001d043767* (*DCD2*), 1.64 and 1.07 in M17-45-1 leaves, 1.54 and 1.07 in M17-5-3 leaves (Figure 7B,C). These results indicate that NaCl stress and exogenous NaHS application are associated with the upregulation of H_2S biosynthesis-related genes in maize seedlings at the transcriptional level. However, because transcript abundance does not necessarily reflect enzyme activity or H_2S biosynthetic flux, these findings should be interpreted as transcriptional associations rather than as evidence of increased H_2S biosynthesis capacity or enhanced salt tolerance, unless supported by enzyme activity assays or functional validation.

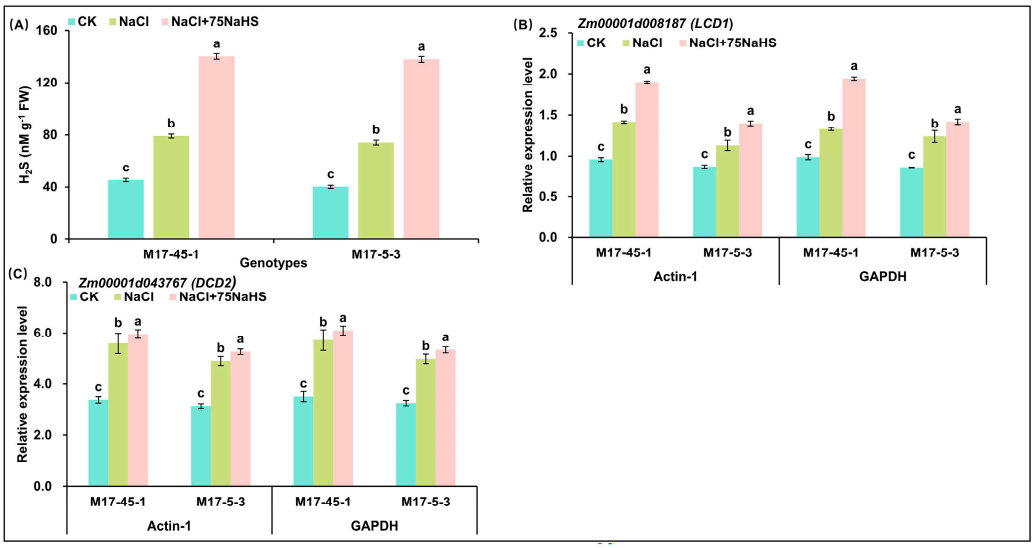

Figure 7. The changes in endogenous hydrogen sulfide (H_2S) content and H_2S biosynthesis-related gene expression levels in the leaves of the seedlings of two maize genotypes (M17-45-1 and M17-5-3) under different treatments. (**A**) Changes in H_2S content. (**B**) *Zm00001d008187* (*LCD1*) expression level using the selected reference genes, including *Zm00001d010159* (*Actin-1*) and *Zm00001d049641* (*GAPDH*). (**C**) *Zm00001d043767* (*DCD2*) expression level using the selected reference genes, including *Zm00001d010159* (*Actin-1*) and *Zm00001d049641* (*GAPDH*). Different lowercase letters indicate significant differences among various treatments within the same maize genotype according to ANOVA at the $p < 0.05$ level, respectively.

3.7. Pearson Correlation Among All Measured Traits and Gene Expression Levels

To better understand the intrinsic relationships among all measured traits and key regulating genes in seedlings of the two maize genotypes, Person correlation analysis was performed under the three treatments. A total of 211 significant ($p < 0.01$ or $p < 0.05$) positive/negative correlations were detected among the measured traits and key regulating genes (Figure 8). This indicates a complex relationship framework between seedling traits and gene expression in maize under different treatments, although such correlations do not by themselves establish causality. Of particular note, endogenous H_2S content was significantly and positively correlated with RFW ($r = 0.57$ *; * represents $p < 0.05$ level), SPAD value ($r = 0.67$ **; ** represents $p < 0.01$ level), Chl a content ($r = 0.57$ *), Chl b content ($r = 0.52$ *), Car content ($r = 0.47$ *), Tr ($r = 0.62$ **), Ci ($r = 0.62$ **), SOD activity ($r = 0.63$ **), POD activity ($r = 0.66$ **), CAT activity ($r = 0.60$ **), and APX activity ($r = 0.53$ **), while significantly and negatively correlating with H_2O_2 content ($r = -0.62$ **; Figure 8), indicating that endogenous H_2S dynamic accumulation is closely correlated with ROS homeostasis, antioxidant enzyme activities, photosynthetic pigment accumulation, photosynthetic performance, and growth status of maize seedlings under the tested conditions. The expression levels of five antioxidant-regulating genes were significantly and positively correlated with the activities of four antioxidant enzymes ($r = 0.52$ *–0.93 **; Figure 8), and the expression levels of two H_2S biosynthesis-related genes were significantly and positively correlated with endogenous H_2S content ($r = 0.82$ **–0.87 **; Figure 8), suggesting that the expression of these genes is closely associated with antioxidant enzyme activities and endogenous H_2S levels in maize seedlings under different conditions.

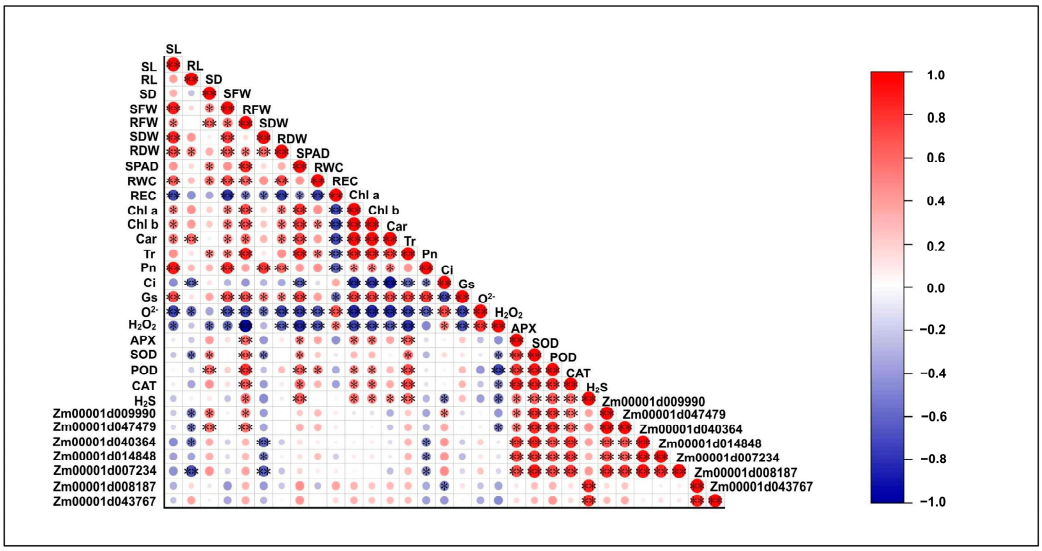

Figure 8. Pearson correlation diagrams of all measured traits and key regulating genes in the two maize genotypes under all treatments. APX: ascorbate peroxidase activity; Chl a: chlorophyll a content; Chl b: chlorophyll b content; Car: carotenoid content; Ci: intercellular CO_2 concentration; CAT: catalase activity; Gs: stomatal conductivity; H_2O_2: hydrogen peroxide content; H_2S: hydrogen sulfide; $O_2^{\bullet-}$: superoxide anion content; Pn: net photosynthetic rate; POD: peroxidase activity; RL: root length; RWC: relative water content; REC: relative electrical conductivity; RFW: root fresh weight; RDW: root dry weight; SL: seedling length; SD: stem diameter; SFW: seedling fresh weight; SDW: shoot dry weight; SPAD: soil plant analysis development; SOD: superoxide dismutase activity; Tr: transpiration rate; *Zm00001d009990* (*SOD3.4*); *Zm00001d047479* (*SOD4A*); *Zm00001d014848* (*CAT1*); *Zm00001d040364* (*POD72*); *Zm00001d007234* (*APX2*); *Zm00001d008187* (*LCD1*); *Zm00001d043767* (*DCD2*). ** or * indicates a significant correlation at the $p < 0.01$ or $p < 0.05$ level, respectively.

4. Discussion

Soil salinity is a major environmental stressor that adversely affects plant health and crop production. In the present study, 120 mM NaCl stress significantly inhibited the growth and photosynthetic performance of maize seedlings and disrupted ROS homeostasis and membrane integrity. Exogenous application of 75 μM NaHS alleviated these adverse effects, with the alleviating effect being more pronounced in M17-5-3 than in M17-45-1. This observation is consistent with previous reports that NaHS can improve salt tolerance in other plant species. For example, 200 μM NaHS improved the ability of cucumber (*Cucumis sativus* L.) seedlings to withstand salt stress by enhancing seedling photosynthesis, promoting the ascorbic acid–glutathione cycle (AsA–GSH), and protecting the absorption of mineral ions under salt stress conditions [42]. Additionally, 100 μM NaHS had also been reported to improve salt tolerance in okra (*Abelmoschus esculentus* L.) by activating the endogenous H_2S-abscisic acid (ABA) regulatory cascade [43]. Other strategies, such as trehalose and melatonin application, have also been shown to alleviate salt stress in celery (*Apium graveolens* L.) and mustard (*Brassica juncea* L.), respectively [44,45]. However, compared with these treatments, NaHS is of particular interest in maize because it is an endogenous gaseous signaling molecule closely linked to sulfur metabolism and antioxidant regulation. Therefore, exploiting saline–alkali soils for stable maize production is an important research goal, and NaHS application may be a promising approach for mitigating salt stress in maize.

Although H_2S has long been regarded as a toxic gas, its potential functions in plants, including both endogenous and exogenous functions, have attracted increasing attention in recent decades [46,47]. At a suitable concentration, exogenous NaHS application can regu-

late diverse physiological processes, including seed germination [48,49], organ formation, and development [50,51], and enhance tolerance to heavy metal poisoning [52,53] and heat stress [54,55]. In plants, endogenous H_2S is produced as an intermediate during sulfate assimilation, with cystathionine β-synthase (CBS), 3-mercaptopyruvate sulfurtransferase (MST), LCD, DCD, cyanoalanine synthase (CAS), and cysteine synthase (CS) implicated in its production [56]. A previous study reported that exogenous salicylic acid (SA) induced endogenous H_2S accumulation, thereby improving maize seed germination under drought stress [57]. In the present study, 75 μM exogenous NaHS significantly upregulated the expression of *LCD1* and *DCD2* and clearly promoted endogenous H_2S accumulation in the leaves of the seedlings of two maize genotypes under 120 mM NaCl stress, consistent with this observation in tobacco seedlings [21]. However, it should be emphasized that the increased transcript abundance of *LCD1* and *DCD2*, together with the elevated H_2S content, constitutes correlative evidence rather than proof of a positive-feedback regulatory mechanism. Establishing such a mechanism would require functional validation, for instance through genetic manipulation or enzyme-activity assays. Accordingly, the present results suggest that exogenous NaHS may stimulate the expression and activity of H_2S synthases (e.g., LCD and DCD), thereby contributing to the elevation of endogenous H_2S levels in plants in diverse environments. Further functional studies are needed to confirm whether this involves a positive-feedback loop.

Applying 75 μM exogenous NaHS significantly decreased leaf $O_2^{\bullet-}$ levels and H_2O_2 content in both maize genotypes under 120 mM NaCl stress, while significantly enhancing leaf SOD, POD, CAT, and APX activities in these maize seedlings. Similar alleviative effects have been reported previously. In aluminum-stressed *Brassica napus* seedlings, 20 μM NaHS mitigated oxidative damage by enhancing antioxidant enzyme activity and proline content [58]. Supplementation with 100 μM NaHS protected mung bean (*Vigna radiata* L.) plants against oxidative stress under 90 μM chromium stress, coinciding with greater cell viability [52]. Application of 0.5 mM NaHS alleviated low-temperature stress in pepper seedlings by improving plasma membrane stability, decreasing $O_2^{\bullet-}$ and malondialdehyde levels, and increasing antioxidant activity [59]. These observations are therefore consistent with the view that an appropriate concentration of NaHS can attenuate oxidative damage and help maintain cellular structural and functional integrity under adverse environmental conditions. We also observed that 75 μM exogenous NaHS clearly upregulated the expression of five antioxidant-regulating genes in leaves of both maize genotypes. In line with our results, Guo et al. [60] reported that cadmium stress increased antioxidative enzyme activities and the relative expression of stress-related genes, including *SOD*, *CAT*, *APX*, *glutathione reductase* (*GR*), *phytochelatin synthase* (*PCS*), and *metallothioneins* (*MT1A*, *MT2A*, and *MT2B*), in *Salix matsudana* Koidz seedlings, and that these responses were further enhanced by 50 mg/kg NaHS supplementation. It should be noted, however, that the relationship between antioxidant enzyme activities and oxidative stress is not always proportional. In the present study, although antioxidant enzyme activities were increased by NaHS treatment in both maize genotypes, some reductions in ROS levels did not reach statistical significance in M17-45-1. Several factors may account for this. First, enzyme activity measured in vitro does not necessarily reflect the net ROS-scavenging capacity in vivo, because ROS homeostasis also depends on non-enzymatic antioxidants (e.g., ascorbate, glutathione, proline) [27], on the balance between ROS production and elimination, and on the subcellular compartment in which ROS are generated. Second, the magnitude of the NaHS effect may differ among genotypes. Specifically, M17-45-1 may have a higher basal antioxidant capacity or a different ROS-scavenging threshold, such that the additional enzyme induction results in a smaller, statistically non-significant net change in ROS.

In addition, this study observed that an imbalance in ROS production was associated with a reduced photosynthetic pigment content and photosynthetic capacity in both maize genotypes under 120 mM NaCl stress. Supplementation with 75 μM exogenous NaHS significantly increased leaf Chl a, Chl b, and Car contents, as well as Pn, in both maize genotypes under 120 mM NaCl stress. In tomato seedlings, Ba et al. [61] similarly reported that 100 μM NaHS increased leaf Chl a, Chl b, and total Chl contents, together with Gs, Pn, and Tr. These results indicate that 75 μM exogenous NaHS can alleviate the adverse effects of NaCl stress on photosynthetic pigments and thereby improve photosynthetic efficiency, which may partly explain the more rapid growth of maize seedlings under NaHS treatment. Additionally, a previous study reported chloroplast abnormalities in leaf cells of tea plants (*Camellia sinensis* L.) under cadmium stress, whereas leaf cells treated with 100 μM NaHS plus cadmium showed a largely intact structure, with visible periplasm and tighter stromal lamellae, and their chloroplast structure differed only slightly from the control [62]. Moreover, early application of exogenous NaHS was reported to alleviate salinity stress in *Cyclocarya paliurus* by effectively maintaining chlorophyll fluorescence [63]. Taken together, these observations are consistent with the interpretation that exogenous NaHS helps preserve photosynthetic pigment content and photosynthetic performance under stress. However, it should be emphasized that the present study measured pigment contents and photosynthetic parameters but did not examine chloroplast ultrastructure, chlorophyll biosynthetic enzymes, or pigment degradation pathways. Accordingly, the present data do not allow us to conclude that NaHS maintains chloroplast structure or promotes chlorophyll biosynthesis.

Concomitantly, excessive salinity can induce ionic toxicity through the accumulation of Na^+ and Cl^- in plant cells [64]. Recent studies have shown that the application of 50 μM NaHS significantly restricted Na^+ uptake while increasing K^+ uptake, thereby preventing a decrease in the Na^+/K^+ ratio in roots, shoots, leaves, and whole seedlings of rice and wheat [65,66]. In the present study, 75 μM NaHS appeared to alleviate salt-induced toxic effects, as evidenced by the levels of H_2O_2, $O_2^{\bullet -}$, and REC, as well as by the phenotypes of the maize seedlings. However, the concentrations of Na^+, K^+, and Cl^- in different tissues of the maize seedlings were not measured, which constitutes a limitation of the present study. This omission is important because ionic toxicity is a major component of salinity stress, and it restricts the interpretation of our results in several respects. This limitation will make it difficult to determine whether the alleviative effect of NaHS are attributed to improved ionic homeostasis or to antioxidant-/photosynthesis-associated responses.

Based on the present results and previously published studies, we propose a response mechanism by which exogenous 75 μM NaHS enhances the salt tolerance of maize (Figure 9). In summary, under 120 mM NaCl stress, supplementation with 75 μM exogenous NaHS effectively alleviated salt injury in the maize genotypes examined; however, the alleviating effect of NaHS varied among genotypes. In the future, the effects of exogenous NaHS on Na^+, K^+, and Cl^- concentrations in maize seedlings under NaCl stress should be examined via atomic absorption spectrometry, and the underlying molecular mechanism and key candidate genes should be further analyzed in maize under combined NaCl and NaHS treatments using high-throughput transcriptome sequencing, thereby facilitating the molecular improvement of salt tolerance in maize. More importantly, the present study has clear limitations that must be emphasized. The experiments were conducted using only two maize genotypes under controlled environmental conditions, and reproductive growth, grain yield, and field-level salinity tolerance were not assessed. Consequently, the practical applicability of 75 μM NaHS in the field remains uncertain, and the present findings should not be extrapolated to field conditions or to maize production without further validation. Field trials are therefore necessary to verify the protective effects of

NaHS on maize under saline–alkali stress, and such trials should ideally include multiple genotypes, reproductive-stage, and yield-related traits, as well as measurements under naturally saline–alkali field conditions, with the aim of providing a theoretical basis and technical support for the safe production of maize in saline–alkali soils.

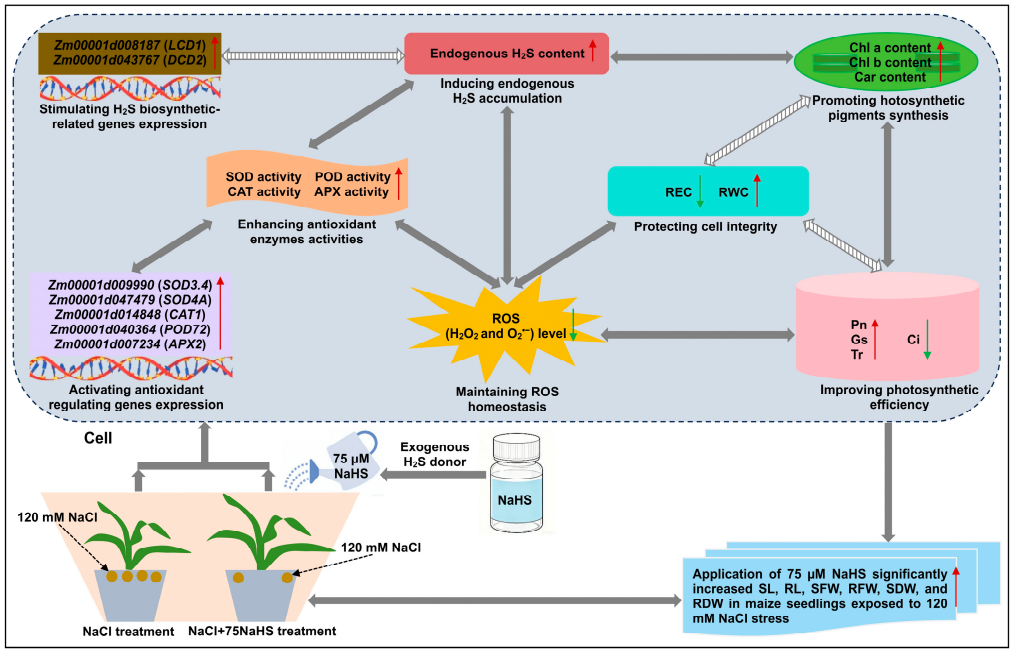

Figure 9. Exogenous H_2S-mediated NaCl stress responses in maize seedlings. APX: ascorbate peroxidase activity; Chl a: chlorophyll a content; Chl b: chlorophyll b content; Car: carotenoid content; CAT: catalase activity; Ci: intercellular CO_2 concentration; Gs: stomatal conductivity; H_2O_2: hydrogen peroxide content; $O_2^{\bullet-}$: superoxide anion content; POD: peroxidase activity; Pn: net photosynthetic rate; RL: root length; REC: relative electrical conductivity; RFW: root fresh weight; RWC: relative water content; SL: seedling length; SFW: seedling fresh weight; SOD: superoxide dismutase activity; Tr: transpiration rate. The red and green arrows indicate increases and decreases in the corresponding traits, respectively. Solid arrows represent measured responses, while dashed arrows represent proposed mechanisms requiring further validation.

5. Conclusions

In summary, this study showed that exogenous application of 75 μM NaHS effectively alleviates salt injury in maize seedlings under 120 mM NaCl stress. This alleviation is accompanied by, and is consistent with, the activation of endogenous H_2S-related responses, the enhancement of antioxidant defense, the accumulation of photosynthetic pigments, and the maintenance of photosynthetic efficiency. Therefore, these findings provide a basis for further investigation and technical reference for maize production in saline–alkali soils, while their field applicability requires verification in field trials.

Supplementary Materials: The following supporting information can be downloaded at: https://www.mdpi.com/article/10.3390/cimb48121289/s1.

Author Contributions: Conceptualization, X.Z.; methodology, X.Z.; analysis, X.X.; investigation, X.X., M.H., J.W., J.L. and S.Y.; resources, X.Z.; writing–original draft preparation, X.X. and X.Z.; writing—review and editing, X.Z.; supervision, X.Z.; acquisition, X.Z.; project administration, X.Z.; funding acquisition, X.Z. All authors have read and agreed to the published version of the manuscript.

Funding: This research was supported by the Project of Gansu Provincial Joint Fund, China (26JRRA936); the Open Research Fund of the State Key Laboratory of Crop Genetics & Germplasm Enhancement and Utilization, Nanjing Agricultural University, China (Z622025011); the Gansu Province

Longyuan Qingnian Yingcai Project, China (LYYC-2025–04); the Fuxi Yong Talent Foundation of Gansu Agricultural University, China (Gaufx-05Y08); the National Natural Science Foundation of China (32360478, 32060486); the Youth Mentor Support Fund of Gansu Agricultural University, China (GAU-QDFC 2024-19); and the Horizontal Project of Gansu Agricultural University, China (GSAU-JSXK-2025-006, GSAU-JSXK-2026-007).

Institutional Review Board Statement: Not applicable.

Informed Consent Statement: Not applicable.

Data Availability Statement: The raw data supporting the conclusions of this article will be made available by the authors on request.

Acknowledgments: We would like to thank the staff at the Longxi experimental stations, Gansu, China, for providing the maize materials.

Conflicts of Interest: The authors declare no conflicts of interests.

Abbreviations

The following abbreviations are used in this manuscript:

APX	ascorbate peroxidase
CAT	catalase
Chl a	chlorophyll a content
Chl b	chlorophyll b content
Car	carotenoid content
Ci	intercellular CO_2 concentration
DCD	D-cysteine desulfhydrase
Gs	stomatal conductance
H_2O_2	hydrogen peroxide
H_2S	hydrogen sulfide
LCD	L-cysteine desulfhydrase
$O_2^{\bullet-}$	superoxide anion
Pn	net photosynthetic rate
POD	peroxidase
RDW	root dry weight
RFW	fresh weight of roots
RL	root length
RWC	relative water content
REC	relative electrical conductivity
SD	stem diameter
SDW	seedling dry weight
SFW	fresh weight of seedlings
SL	seedling length
SPAD	relative chlorophyll content
SOD	superoxide dismutase
Tr	transpiration rate

References

1. Wen, W.; Cheng, L.X.; Zou, Y.Y.; Wang, C.; Zhang, X.M.; Gao, Y.J.; Cui, J.L.; Gu, B.J. Global management of saline soils to boost crop yields and halve nitrogen losses. *Nat. Food* **2026**, *7*, 974–985. [CrossRef] [PubMed]
2. Sun, S.Q.; Zhao, X.Q.; Li, X.; He, M.Y.; Wang, J.; Xiang, X.X.; Niu, Y.N. ZnONPs alleviates salt stress in maize seedlings by improving antioxidant defense and photosynthesis potential. *Plants* **2025**, *14*, 3104. [CrossRef] [PubMed]
3. Mittle, R.; Zandalinas, S.I.; Fichman, Y.; Breusegsm, F.V. Reavtive oxygen species signalling in plant stress responses. *Nat. Rev. Mol. Cell Biol.* **2022**, *23*, 663–679. [CrossRef] [PubMed]
4. Omar, A.A.A.; Zaman, M.M.U.; Abedin, M.T.; Alam, M.S.; Khatun, M.A.; Akter, N.; Sayed, M.A. Unraveling the dynamics of salt stress response in wheat cultivars: Insights into growth inhibition, antioxidant enzyme activity, and AOX gene expression. *J. Crop Sci. Biotechnol.* **2024**, *27*, 439–448. [CrossRef]
5. Yang, X.X.; Shi, Q.F.; Wang, X.R.; Zhang, T.; Feng, K.; Wang, G.; Zhao, J.; Yuan, X.Y.; Ren, J.H. Melatonin-Induced chromium tolerance requires hydrogen sulfide signaling in maize. *Plants* **2024**, *13*, 1763. [CrossRef] [PubMed]

6. Zhang, Z.L.; Liu, R.; Zong, X.X.; Zheng, X.P.; Yang, T. Comprehensive evaluation of salt tolerance in broad beans at different growth stages and study on the relief of salt stress during germination period by isocitric acid. *Sci. Agric. Sin.* **2026**, *59*, 1172–1188.
7. Li, G.H.; Guo, X.; Sun, Y.N.; Zhao, H.L.; Zhao, H.J.; Wang, X.J.; Fu, C.; Zhao, C.Z. The content of flavonoids and the activity of antioxidant enzymes in different peanut varieties under salt stress. *Chin. J. Oil Crop Sci.* **2023**, *45*, 803–809.
8. Sadak, M.S.; Abd El-Monem, A.A.; El-Bassiouny, H.M.S.; Badr, N.M. Physiological response of sunflower (*Helianthus annuus* L.) to exogenous arginine and putrescine treatments under salinity stress. *J. Appl. Sci. Res.* **2012**, *8*, 4943–4957.
9. Xu, Y.M.; Bu, W.C.; Xu, Y.C.; Fei, H.; Zhu, Y.M.; Ahmad, I.; Ahmed, N.E.; Zhou, G.S.; Zhu, G.L. Effects of salt stress on physiological and agronomic traits of rice genotypes with contrasting salt tolerance. *Plants* **2024**, *13*, 1157. [CrossRef] [PubMed]
10. Ulrike, G.; Anja, F.; Thanh, T.N.; Olaf, E. Food security and the dynamics of wheat and maize Value chains in Africa and Asia. *Front. Sustain. Food Syst.* **2021**, *4*, 617009. [CrossRef]
11. Khalil, A.G.; Bassuony, F.M.; Haroun, S.A.; Khalil, R.R. Effect of different concentrations of sodium chloride, sodium selenate, alpha-tocopherol and ascorbic acid each one alone on germination and growth of maize plant. *Benha J. Appl. Sci.* **2021**, *6*, 156–162. [CrossRef]
12. Sun, M.K.; Li, C.H.; Li, H.; Yang, B.L.; Deng, Y.; Li, Y.H.; Ma, F.Y.; Wang, X.Y.; He, F.; Guo, L.C.; et al. Effects of NaCl and $NaHCO_3$ stress on seed germination of winter rye. *J. Anhui Agric. Sci.* **2024**, *52*, 28–33.
13. Wang, Y.; Gu, W.; Meng, Y.; Xie, T.; Li, L.; Li, J.; Wei, S. γ-Aminobutyric acid imparts partial protection from salt stress injury to maize seedlings by improving photosynthesis and upregulating osmoprotectants and antioxidants. *Sci. Rep.* **2017**, *7*, 43609. [CrossRef] [PubMed]
14. Liu, X.T.; Yao, T.; Chai, J.L.; Han, J.R. Adsorption of sodium ions by exopolysaccharides from pseudomonas simiae MHR6 and its improving of Na^+/K^+ homeostasis in maize under salt stress. *Agric. Food Chem.* **2023**, *71*, 49–57. [CrossRef] [PubMed]
15. Luo, Y.; Zeng, W.Z.; Lei, G.Q.; Hou, Y.L.; Ao, C.; Chen, H.R.; Gaiser, T.; Srivastava, A.K. The effects of multiwalled carbon nanotubes and Bacillus subtilis treatments on the salt tolerance of maize seedlings. *Front. Plant Sci.* **2022**, *13*, 1093529. [CrossRef] [PubMed]
16. Shelke, D.B.; Pandey, M.; Nikalje, G.C.; Zaware, B.N.; Suprasanna, P.; Nikam, T.D. Salt responsive physiological, photosyn thetic and biochemical attributes at early seedling stage for screening soybean genotypes. *Plant Physiol. Biochem.* **2017**, *118*, 519–528. [CrossRef] [PubMed]
17. Xuan, L.J.; Wang, X.Y.; Wang, C.Y. Crosstalk between hydrogen sulfide and other signal molecules regulates plant growth and development. *Int. J. Mol. Sci.* **2020**, *21*, 4593. [CrossRef] [PubMed]
18. Wang, C.L.; Deng, Y.Z.; Liu, Z.S.; Liao, W.B. Hydrogen sulfide in plants: Crosstalk with other signal molecules in response to abiotic stresses. *Int. J. Mol. Sci.* **2021**, *22*, 12068. [CrossRef] [PubMed]
19. Daneshvand, E.; Rahmani, F.; Abbaspour, N.; Rahimi, A. Hydrogen sulfide's role in enhancing antioxidant defense and biochemical resilience in salt-stressed lavender (*Lavandula angustifolia*) Plants. *Russ. J. Plant Physiol.* **2025**, *72*, 15. [CrossRef]
20. Zhang, H.; Hu, L.Y.; Hu, K.D.; He, Y.D.; Wang, S.H.; Luo, J.P. Hydrogen sulfide promotes wheat seed germination and alleviates oxidative damage against copper stress. *J. Integr. Plant Biol.* **2008**, *12*, 1518–1529. [CrossRef] [PubMed]
21. Dai, J.C.; Wen, D.X.; Li, H.; Yang, J.P.; Rao, X.F.; Yang, Y.; Yang, J.K.; Yang, C.L.; Yu, J. Effect of hydrogen sulfide (H_2S) on the growth and development of tobacco seedlings in absence of stress. *BMC Plant Biol.* **2024**, *24*, 162. [CrossRef] [PubMed]
22. Yang, L.; Yang, J.H.; Hou, C.X.; Shi, P.P.; Zhang, Y.W.; Gu, X.L.; Liu, W.Z. Hydrogen sulfide alleviates salt stress through auxin signaling in *Arabidopsis*. *Environ. Exp. Bot.* **2023**, *211*, 105354. [CrossRef]
23. Zhao, X.Q.; Sun, S.Q.; Niu, Y.N.; Li, X.; He, M.Y.; Wang, J.; Xiang, X.X.; Long, J.M.; Gao, X.Q. Graphene oxide nanoparticles boost growth development, grain anthocyanins accumulation and coloration formation of purple waxy maize under polyvinyl chloride microplastics stress. *J. Hazard. Mater.* **2026**, *503*, 14123. [CrossRef] [PubMed]
24. Sonmez, D.A.; Akbari, A.; Yesil, B.; Kafkas, S.; Mezzetti, B.; Kafkas, N.E. A comprehensive analysis of the physiological and biochemical responses of raspberry cultivars to water stress. *Sci. Rep.* **2025**, *15*, 43707. [CrossRef] [PubMed]
25. Khampookhiaw, N.; Khianpho, O.; Santanoo, S.; Pamuta, D.; Theerakulpisut, P. Slat tolerance and physiological responses at the seedong, vegetative, and reproductive stages of thai jasmine rice KDML105 and its genetically improved variety (RD73) and line (TSKC1-144). *Plants* **2026**, *15*, 2635. [CrossRef] [PubMed]
26. He, F.Q.; Zhao, X.Q.; Qi, G.X.; Sun, S.Q.; Shi, Z.Z.; Niu, Y.N.; Wu, Z.F. Exogenous melatonin alleviates NaCI injury by influencing stomatal morphology, photosynthetic performance, and antioxidant balance in maize. *Int. J. Mol. Sci.* **2024**, *25*, 10077. [CrossRef] [PubMed]
27. Zhao, X.Q.; Niu, Y.N.; Chao, W.; He, W.; Wang, Y.F.; Mao, T.T.; Bai, X.D. Understanding and comprehensive evaluation of cold Resistance in the seedlings of multiple maize genotypes. *Plants* **2022**, *11*, 1881. [CrossRef] [PubMed]
28. Zhao, X.Q.; Sun, S.Q.; Li, X.; Niu, Y.N.; Gao, X.Q. The effects of polyvinyl chloride microplastics and zinc oxide nanoparticles co-exposure on nutritional quality of purple waxy maize grains. *Food Chem.* **2025**, *496*, 146759. [CrossRef] [PubMed]

29. Zhao, X.Q.; Li, J.Y.; Niu, Y.N.; Hossain, Z.; Gao, X.Q.; Bai, X.D.; Mao, T.T.; Qi, G.X.; He, F.Q. Exogenous serotonin (5-HT) promotes mesocotyl and coleoptile elongation in maize seedlings under deep-seeding stress through enhancing auxin accumulation and inhibiting lignin formation. *Int. J. Mol. Sci.* **2023**, *24*, 17061. [CrossRef] [PubMed]
30. Lin, Y.A.; Zhang, C.L.; Lan, H.; Gao, S.B.; Liu, H.L.; Liu, J.; Cao, M.J.; Pan, G.T.; Rong, T.Z.; Zhang, S.Z. Validation of potential reference genes for qPCR in maize across abiotic stresses, hormone treatments, and tissue types. *PLoS ONE* **2014**, *9*, 445. [CrossRef] [PubMed]
31. Keyster, M.; Klein, A.; Du Plessis, M.; Jacobs, A.; Kappo, A.; Kocsy, G.; Galiba, G.; Ludidi, N. Capacity to control oxidative stress-induced caspase-like activity determines the level of tolerance to salt stress in two contrasting maize genotypes. *Acta Physiol. Plant.* **2013**, *35*, 31–40. [CrossRef]
32. Roy, T.K.; Islam, M.S.; Antu, U.B.; Sumi, M.J.; Irin, I.J.; Hossain, S.A.; Akter, K.; Mazrin, M.; Mahiddin, N.A.; Meem, H.Z.; et al. Exogenous application of ZnO nanoparticles (NPs) to palliate salinity induced oxidative stress in lettuce (*Lactuca sativa* L.) plant. *J. Soil Sci. Plant Nutr.* **2025**, *25*, 6398–6412. [CrossRef]
33. Li, X.; Zhang, W.; Niu, D.; Liu, X.M. Effects of abiotic stress on chlorophyll metabolism. *Plant Sci.* **2024**, *342*, 112030. [CrossRef] [PubMed]
34. Simkin, A.J.; Kapoor, L.; Doss, C.G.P.; Hofmann, T.A.; Lawson, T.; Ramamoorthy, S. The role of photosynthesis related pigments in light harvesting, photoprotection and enhancement of photosynthetic yield in planta. *Photosynth. Res.* **2022**, *152*, 23–42. [CrossRef] [PubMed]
35. Yong, S.; Chen, Q.; Xu, F.; Fu, H.; Liang, G.; Guo, Q. Exploring the interplay between angiosperm chlorophyll metabolism and environmental factors. *Planta* **2024**, *260*, 25. [CrossRef] [PubMed]
36. Duo, Y.X.; Wu, Z.G.; Dai, J.F.; Yang, Y.; Zhang, L.S. Sodium hydrosulfide (NaHS) triggers jasmonate and Reactive Oxygen Species to Boost Rice (*Oryza sativa* L.) Growth, Flowering, and grain yield. *Plants* **2026**, *15*, 1438. [CrossRef] [PubMed]
37. Khan, S.; Alvi, A.F.; Fatma, M.; Hashimi, A.A.; Sofo, A.; Khan, N.A. Relative effects of melatonin and hydrogen sulfide treatments in mitigating salt damage in wheat. *Front. Plant Sci.* **2024**, *15*, 1406092. [CrossRef] [PubMed]
38. Tiago, F.J.; Takayuki, T.; Regina, W.; José, C.R.; Fernando, C.L.; Ana, I.R.; Alisdair, R.F.; Carla, A. Salt-stress secondary metabolite signatures involved in the ability of Casuarina glauca to mitigate oxidative stress. *Environ. Exp. Bot.* **2019**, *166*, 103808. [CrossRef]
39. Mirza, H.; Md, R.; Hossain, R.; Chowdhury, M.A.A.; Khussboo, R.; Farzana, N.; Mira, R.; Kamrun, N.; Masayuki, F. Regulation of reactive oxygen species and antioxidant defense in plants under salinity. *Int. J. Mol. Sci.* **2021**, *22*, 9326. [CrossRef] [PubMed]
40. Gad, M.; Nobuhiro, S.; Sultan, C.Y.; Ron, M. Reactive oxygen species homeostasis and signalling during drought and salinity stresses. *Plant Cell Environ.* **2010**, *33*, 453–467. [CrossRef] [PubMed]
41. Mo, R.X.; Kang, C.; Yuan, J.P.; Redshaw, C.; Huang, Y.; Zhang, Q.L.; Yan, X.F. A near-infrared ratiometric fluorescent probe for visual sensing of H_2S and monitoring its fluctuation in plant roots under drought and flooding stresses. *Anal. Chim. Acta* **2026**, *1392*, 345144. [CrossRef] [PubMed]
42. Jiang, J.L.; Tian, Y.; Li, L.; Yu, M.; Hou, R.P.; Ren, X.M. H2S alleviates salinity stress in cucumber by maintaining the Na+/K+ balance and regulating H2S metabolism and oxidative stress response. *Front. Plant Sci.* **2019**, *10*, 678. [CrossRef] [PubMed]
43. Wang, F.B.; Chen, X.; Li, N.N.; Pei, B.L.; Chen, X.H.; Ye, Y.X. Exogenous NaHS-derived H_2S allleviates salt stress in okra via H2S-ABA signaling and radox homeostasis. *Plant Soil* **2026**, *529*, 941–966. [CrossRef]
44. Gao, Y.Q.; Zhang, L.M.; Rui, W.J.; Zhang, M.; Liang, Z.X.; Pu, K.G.; Chang, Y.L.; Ma, Y.W.; Huo, J.W.; Zhang, J.J. Regulatory effects of exogenous trehalose on the growth and photosynthetic characteristics of celery (*Apium graveolens* L.) under salt stress. *Plants* **2026**, *15*, 212. [CrossRef] [PubMed]
45. Zhao, X.L.; Yu, X.N.; Di, H.M.; Zhou, A.L.; Guan, Z.G.; Shi, P.P.; Wang, S.; Sun, B. Melatonin enhances growth and glucosinolate-associated nutritional quality of mustard sprouts under moderate salinity stress. *Plants* **2025**, *14*, 3553. [CrossRef] [PubMed]
46. Liu, H.; Wang, J.C.; Liu, J.H.; Liu, T.; Xue, S.W. Hydrogen sulfide (H_2S) signaling in plant development and stress responses. *aBIOTECH* **2021**, *2*, 32–63. [CrossRef] [PubMed]
47. Yang, M.; Qin, B.P.; Ma, X.L.; Wang, P.; Li, M.L.; Chen, L.L.; Sun, A.Q.; Wang, Z.L.; Yin, Y.P. Foliar application of sodium hydrosulfide (NaHS), a hydrogen sulfide(H_2S) donor, can protect seedlings against heat stress in wheat (*Triticum aestivum* L.). *J. Integr. Agric.* **2016**, *15*, 2745–2758. [CrossRef]
48. Zhang, J.; Liang, X.N.; Xie, S.M.; Liang, Y.; Liang, S.; Zhou, J.; Huang, Y. Effects of hydrogen sulfide on the growth and physiological characteristics of Miscanthus sacchariflorus seedlings under cadmium stress. *J. Ecotoxicol. Environ. Saf.* **2023**, *263*, 115281. [CrossRef] [PubMed]
49. Chen, Z.; Yang, B.F.; Hao, Z.K.; Zhu, J.Q.; Zhang, Y.; Xu, T.T. Exogenous hydrogen sulfide ameliorates seed germination and seedling growth of cauliflower under lead stress and its antioxidant role. *J. Plant Growth Regul.* **2018**, *37*, 5–15. [CrossRef]
50. Fang, T.; Cao, Z.Y.; Li, J.L.; Shen, W.B.; Huang, L.Q. Auxin-induced hydrogen sulfide generation is involved in lateral root formation in tomato. *Plant Physiol. Biochem.* **2014**, *76*, 44–51. [CrossRef] [PubMed]
51. Zhang, H.; Tang, J.; Liu, X.P.; Wang, Y.; Yu, W.; Peng, W.Y.; Fang, F.; Ma, D.F.; Wei, Z.J.; Hu, L.Y. Hydrogen sulfide promotes root organogenesis in ipomoea batatas, salix matsudana and glycine max. *Integr. Plant Biol.* **2009**, *51*, 1086–1094. [CrossRef] [PubMed]

52. Deepti, S.; Lal, N.S.; Dharmendra, S.; Manzer, H.S.; Jyoti, T.; Kumar, S.S.; Abhishek, R.; Kumar, S.C.; Abdullah, A.A.; Saleh, A. Exogenous hydrogen sulfide alleviates chromium toxicity by modulating chromium, nutrients and reactive oxygen species accumulation, and antioxidant defence system in mungbean (*Vigna radiata* L.) seedlings. *Plant Physiol. Biochem.* **2023**, *200*, 107767. [CrossRef] [PubMed]
53. Xiang, Z.X.; Li, W.; Lu, Y.T.; Yuan, T.T. Hydrogen sulfide alleviates osmotic stress-induced root growth inhibition by promoting auxin homeostasis. *Plant J.* **2023**, *114*, 1369–1384. [CrossRef] [PubMed]
54. Kharbech, O.; Massoud, M.B.; Sakouhi, L.; Djebali, W.; Mur, L.A.J.; Chaoui, A. Exogenous application of hydrogen sulfide reduces chromium toxicity in maize seedlings by suppressing NADPH oxidase activities and methylglyoxal accumulation. *Plant Physiol. Biochem.* **2020**, *154*, 646–656. [CrossRef] [PubMed]
55. Zhang, X.W.; Fu, X.; Liu, F.J.; Wang, Y.N.; Bi, H.G.; Ai, X.Z. Hydrogen sulfide improves the cold stress resistance through the *CsARF5-CsDREB3* module in cucumber. *Int. J. Mol. Sci.* **2021**, *22*, 13229. [CrossRef] [PubMed]
56. Zhu, C.Q.; Wei, Q.Q.; Hu, W.J.; Kong, Y.L.; Xiang, X.J.; Zhang, H.; Cao, X.C.; Zhu, L.F.; Liu, J.; Tian, W.H. Unearthing the alleviatory mechanisms of hydrogen sulfide in aluminum toxicity in rice. *Plant Physiol. Biochem.* **2022**, *182*, 133–144. [CrossRef] [PubMed]
57. Tu, M.X.; Zhou, H.D.; Luo, X.P.; Mao, C.Y.; Li, Z.G. Salicylic acid-triggered hydrogen sulfide improves maize seed germination under drought stress by bolstering osmoregulatory system. *Plant Cell Rep.* **2025**, *44*, 246. [CrossRef] [PubMed]
58. Yu, Y.; Dong, J.; Li, R.; Zhao, X.; Zhu, Z.H.; Zhang, F.G.; Zhou, K.J.; Lin, X.Y. Sodium hydrosulfide alleviates aluminum toxicity in brassica napus through maintaining H_2S, ROS homeostasis and enhancing aluminum exclusion. *Sci. Total Environ.* **2023**, *858*, 160073. [CrossRef] [PubMed]
59. Song, X.P.; Zhu, L.; Wang, D.; Liang, L.; Xiao, J.C.; Tang, W.; Xie, M.H.; Zhao, Z.; Lai, Y.S.; Sun, B. Molecular regulatory mechanism of exogenous hydrogen sulfide in alleviating low-temperature stress in pepper seedlings. *Int. J. Mol. Sci.* **2023**, *24*, 16337. [CrossRef] [PubMed]
60. Guo, L.; Ling, L.; Wang, X.Q.; Cheng, T.; Wang, H.Y.; Ruan, Y.N. Exogenous hydrogen sulfide and methylglyoxal alleviate cadmium-induced oxidative stress in Salix matsudana koidz by regulating glutathione metabolism. *BMC Plant Biol.* **2023**, *23*, 73. [CrossRef] [PubMed]
61. Ba, Y.R.; Zhai, J.L.; Yan, J.P.; Li, K.Z.; Xu, H.N. H_2S improves growth of tomato seedlings involving the MAPK signaling. *Sci. Hortic.* **2021**, *288*, 110366. [CrossRef]
62. Xing, A.Q.; Dai, L.C.; Zhang, Y.; Sui, X.Y.; Wu, Z.C.; Wan, S.; Liu, S.J.; Chen, X.; Li, X.H.; Wang, Y.H. Application of exogenous hydrogen sulfide alleviates cadmium-induced stress on tea plant growth. *Plant Stress* **2025**, *17*, 100968. [CrossRef]
63. Chen, P.; Yang, W.X.; Wen, M.X.; Jin, S.H.; Liu, Y. Hydrogen sulfide alleviates salinity stress in cyclocarya paliurus by maintaining chlorophyll fluorescence and regulating nitric oxide level and antioxidant capacity. *Plant Physiol. Biochem.* **2021**, *167*, 738–747. [CrossRef] [PubMed]
64. Gupta, B.; Huang, B.R. Mechanism of salinity tolerance in plants: Physiological, biochemical, and molecular characterization. *Int. J. Genom.* **2014**, *1*, 18. [CrossRef] [PubMed]
65. Mostofa, M.G.; Saegusa, D.; Fujita, M.; Tran, L.P. Hydrogen sulfide regulates salt tolerance in rice by maintaining Na^+/K^+ balance, mineral homeostasis and oxidative metabolism under excessive salt stress. *Front. Plant Sci.* **2015**, *6*, 1055. [CrossRef] [PubMed]
66. Deng, Y.Q.; Bao, J.; Yuan, F.; Liang, X.; Feng, Z.T.; Wang, B.S. Exogenous hydrogen sulfide alleviates salt stress in wheat seedlings by decreasing Na^+ content. *Plant Growth Regul.* **2016**, *79*, 391–399. [CrossRef]

Disclaimer/Publisher's Note: The statements, opinions and data contained in all publications are solely those of the individual author(s) and contributor(s) and not of MDPI and/or the editor(s). MDPI and/or the editor(s) disclaim responsibility for any injury to people or property resulting from any ideas, methods, instructions or products referred to in the content.